Bioactive metabolites of endophytic fungi of the Mexican yew (Taxus globosa) and the isolation and chemical modification of sphaeric acid
by Royce Allen Wilkinson

A thesis submitted in partial fulfillment of the requirements for the degree of Doctor of Philosophy in Chemistry
Montana State University

Abstract:
Over the past decade there has been an increase in the need for novel pharmaceuticals. The development of microbial resistance to current clinical antibiotics, and the increasing number of immunocompromised hosts (AIDS patients, patients on chemotherapy, etc.) are two major reasons new antibiotics are required. New antitumor compounds with greater efficacy and fewer side effects are also in demand.

Endophytic microbes, fungi and bacteria living within the intercellular spaces of higher plants, are one possible source of novel bioactive compounds which are mostly unexplored. The endophytic microbes of yew trees were studied as a novel source of the antitumor drug, taxol, and the collection of microbes isolated in the search for taxol are also being screened for novel bioactive metabolites.

Epicorazine A, a previously known isolate of the fungus, Epicoccum nigrum, with wide spectrum antibiotic activity, was isolated and characterized. Additionally, a novel succinic acid derivative, sphaeric acid, was isolated from a fungus identified as a Sphaeriopsis sp.

Several synthetic modifications of the acid functionalities of sphaeric acid were carried out to explore any structure/function relationships. These modifications included esterifications, amidifications, a reduction, and a subsequent oxidation. A variety of activities were observed among the derivatives in each of the bioassays. However, few consistent trends Were observed throughout the entire range of assays.

Finally, the effect of various culture media on bioactive metabolite production was studied. Several possible bioactive fractions were observed. Succinic acid was isolated as one of the active fractions, and a mixture of triacylglycerols were isolated due to their physical and spectroscopic similarities to sphaeric acid. Several active fractions remain that have the potential of yielding novel bioactive metabolites.

BIOACTIVE METABOLITES OF ENDOPHYTIC FUNGI OF THE MEXICAN YEW (*TAXUS GLOBOSA*) AND THE ISOLATION AND CHEMICAL MODIFICATION OF SPHAERIC ACID

by

Royce Allen Wilkinson

A thesis submitted in partial fulfillment
of the requirements for the degree

of

Doctor of Philosophy

in

Chemistry

MONTANA STATE UNIVERSITY
Bozeman, Montana

January 1998

APPROVAL

of a thesis submitted by

Royce Allen Wilkinson

This thesis has been read by each member of the thesis committee and has been found to be satisfactory regarding content, English usage, format, citations, bibliographic style, and consistency, and is ready for submission to the College of Graduate Studies.

Dr. Arnold C. Craig — Arnold C Craig (Signature) — Jan. 12, 1998 (Date)

Approved for the Department of Chemistry

Dr. David M. Dooley — David M Dooley (Signature) — _____ (Date)

Approved for the College of Graduate Studies

Dr. Joseph J. Fedock — Joseph J. Fedock (Signature) — 1/15/98 (Date)

STATEMENT OF PERMISSION TO USE

In presenting this thesis in partial fulfillment of the requirements for a doctoral degree at Montana State University-Bozeman, I agree that the Library shall make it available to borrowers under the rules of the Library. I further agree that copying of this thesis is allowable only for scholarly purposes, consistent with "fair use" as prescribed in the U.S. Copyright Law. Requests for extensive copying or reproduction of this thesis should be referred to University Microfilms International, 300 North Zeeb Road, Ann Arbor, Michigan 48106, to whom I have granted "the exclusive right to reproduce and distribute my dissertation in and from microform along with the non-exclusive right to reproduce and distribute my abstract in any format in whole or in part."

Signature 

Date 1/13/98

ACKNOWLEDGEMENTS

I wish to thank all my advisors, Dr. Andrea Stierle, Dr. Gary Strobel, and Dr. Arnold Craig, for their support and guidance along the way. I appreciate the flexibilty that they demonstrated in allowing me to work on this interdisciplinary thesis, and for giving me the freedom to chart my own course.

I also wish to thank all of those who supported this work and helped in various ways: Dr. Bret Neidens for initial fungal isolation, Dr. Gene Ford for fungal identification, Dr. Wm. Hess for the photomicrographs and slides of MA17, Dr. Jon Clardy for X-ray crystal confirmation of epicorazine A, Dr. Joe Sears for mass spectral data, Dr. Scott Busse for assistance on the NMR, and to Rick Torczynski at Cytoclonal Pharmaceuticals and those at Pharmagenesis for additional bioassay data.

Additional thanks to all my friends and family for their support and love. It's not what you accomplish, but the people that you encounter as you go through life, that make it all worth while.

Finally, I must thank my Lord and Savior, Jesus Christ, for all that He has done for me. I am so grateful for the abilities He has given me. I pray that I will be able to use them for His glory. "'For I know the plans I have for you,' declares the Lord, 'plans to prosper you and not to harm you, plans to give you hope and a future.'" Jeremiah 29:11 (NIV).

TABLE OF CONTENTS

LIST OF TABLES

LIST OF FIGURES

ABSTRACT

Over the past decade there has been an increase in the need for novel pharmaceuticals. The development of microbial resistance to current clinical antibiotics, and the increasing number of immunocompromised hosts (AIDS patients, patients on chemotherapy, etc.) are two major reasons new antibiotics are required. New antitumor compounds with greater efficacy and fewer side effects are also in demand.

Endophytic microbes, fungi and bacteria living within the intercellular spaces of higher plants, are one possible source of novel bioactive compounds which are mostly unexplored. The endophytic microbes of yew trees were studied as a novel source of the antitumor drug, taxol, and the collection of microbes isolated in the search for taxol are also being screened for novel bioactive metabolites.

Epicorazine A, a previously known isolate of the fungus, *Epicoccum nigrum*, with wide spectrum antibiotic activity, was isolated and characterized. Additionally, a novel succinic acid derivative, sphaeric acid, was isolated from a fungus identified as a *Sphaeriopsis* sp.

Several synthetic modifications of the acid functionalities of sphaeric acid were carried out to explore any structure/function relationships. These modifications included esterifications, amidifications, a reduction, and a subsequent oxidation. A variety of activities were observed among the derivatives in each of the bioassays. However, few consistent trends were observed throughout the entire range of assays.

Finally, the effect of various culture media on bioactive metabolite production was studied. Several possible bioactive fractions were observed. Succinic acid was isolated as one of the active fractions, and a mixture of triacylglycerols were isolated due to their physical and spectroscopic similarities to sphaeric acid. Several active fractions remain that have the potential of yielding novel bioactive metabolites.

Chapter 1

INTRODUCTION

The Antibiotic Paradox

The "antibiotic paradox" is a phrase coined by Stuart Levy, M.D. describing the fact that antibiotics have sown the seeds of their own downfall by selecting for strains of bacteria that can resist their activity. These "miracle drugs" achieved their great acclaim by rapidly curing previously fatal infections. However, bacteria responded to the widespread use of antibiotics by finding ways of becoming insensitive to the killing effects of these drugs. Beyond this, many of these resistant traits have been found to be transferable from one resistant bacteria to another; even bacteria of different types.[1]

This has become such a concern that even the popular media has covered this phenomenon. *Time* magazine ran a story in 1994 entitled "The Killers All Around" which listed recent outbreaks by new or mutated bacteria and viruses. These included the "flesh eating" streptococcus-A infections in England, a flare-up of tuberculosis in southern California, an epidemic of pertussis (whooping cough) in Cincinnati, and several unknown viral and bacterial illnesses including the Hantavirus outbreak in the southwestern US. As little as a generation ago, medical researchers had begun to believe the end of infectious diseases was

only a matter of time. As *Time* put it, "the question ceased to be, When will diseases be gone? and became, Where will the next deadly virus appear?"[2]

The leading causes of the "antibiotic paradox" have been the widespread use and misuse of these drugs. The use of antibiotics for ailments for which they have no value[3], the sustained use of a single antibiotic[4], and incomplete treatment, that is, stopping the antibiotic treatment before destroying all infectious bacteria[5], have all been factors in decreasing the susceptibility of these pathogens to the current drugs.

The answer to this problem lies not in abolishing the use of antibiotics, but in the wise use of them, as well as the discovery and development of new antibiotics. A new metabolite with a specific mode of action could have a big impact in antibiotic treatments. Even if the activity is insufficient for use as a therapeutic agent, the natural product could be useful as a biochemical tool as either a starting material or as a template for chemical synthesis. A large number of antibacterial compounds have been discovered, but there is still a need for new types of therapeutic agents. The natural mutation of both pathogenic and antibiotic producing organisms will continue to supply both the need and a source for these agents.[6]

Taxol is a classic example of a compound whose novel mode of action inspired tremendous interest. Unlike other antimitotic agents which inhibit microtubule assembly, taxol actually promotes the assembly of tubulin and stabilizes the microtubules so formed.[7] This unique mode of action, coupled

with taxol's particular efficacy against refractory breast and ovarian cancers, has made this one of the most important antitumor agents of the past two decades.[8]

In addition to the need for new antibacterial compounds, antifungal agents are becoming more important as the occurrence of fungal infections increases among immunocompromised hosts. Aging, acquired immunodeficiency syndrome (AIDS), and treatment with immunosuppressive drugs such as anticancer agents are current factors increasing the frequency of opportunistic fungal infections. In many of these cases, the actual cause of death is fungal growth in the organs and blood, rather than tumors or AIDS itself.[9]

Clinically useful antifungal compounds are less common than antibacterial agents for several reasons. First and foremost, fungi are eucaryotes similar to human and animal cells. Therefore, selective toxicity is less likely to occur with antifungal agents. In addition, potent fungicidal effects are desired, but almost all the antifungal drugs now available for use are fungistatic. Those compounds which show strong fungicidal activity are unfortunately also highly cytotoxic. Finally, the host defense system is still a major factor in successful antimicrobial chemotherapy. However, fungal infections are mostly associated with a depression in host immune action making antifungal therapy less effective.[10]

Why Fungi?

The fungi form one of the largest kingdoms of living organisms with a conservatively estimated total of about 1.5 million species. Based on this

estimated figure, only 4.6% of the world's fungi have been recognized, and secondary metabolites have only been documented in about 5000 (or 7%) of the known species.[11] Therefore, a large pool of unknown fungi exists which will likely be found to exhibit novel chemicals among their secondary metabolites.

Two major areas of bioactivity of fungal produced compounds which have precedence in the literature are antibiotic (antifungal and antibacterial) substances and antitumor agents. Amphotericin B is currently the only antifungal compound of microbial origin which is now available for systemic use.[12] It was isolated from a soil actinomycete, *Streptococcus nodosus*, by W. Gold in 1955. Despite its adverse side effects, it remains the standard treatment for most serious mycoses.[13]

Antibacterial agents from microorganisms are a little more common. Penicillin is probably the most celebrated antibiotic. Vancomycin, a fungal derived glycopeptide, is another commonly used antibiotic isolated from a strain of *Streptomyces* (now *Amycolatopsis*) *orientalis* in 1956.[14] There are also several synthetic analogs of microbial compounds used clinically as antibiotics. Included in these are analogs of the monocyclic β-lactams isolated from various soil bacteria and analogs of cephalosporin produced by the fungus *Cephalosporium acremonium*.[15,16] There have been several new antibacterial compounds isolated from microbes over the last few years. Omura's book, *The Search for Bioactive Compounds from Microorganisms*, contains a table of recently isolated compounds which inhibit bacterial cell wall formation. The

table lists 47 compounds (some previously identified) which were published since 1980.[17]

Actinomycin D, mitomycin C, doxorubicin, and bleomycin are among the microbe-derived compounds that are currently being used clinically as antitumor agents.[18] A major discovery in this area was the isolation of the enediyne class of antitumor compounds including calicheamicin and esperamicin by May Lee at the Lederle Laboratories of the American Cyanamid Company. These are some of the most potent agents ever discovered, with calicheamicin being over 1000 times more potent than clinically useful antitumor antibiotics. The calicheamicins are produced by the fermentation of *Micromonospora echinospora* ssp *calichensis*, a bacterium isolated from a soil sample collected in Texas.[19] Omura's book also contains a list of 58 novel antitumor antibiotics isolated from microorganisms since 1984.[20]

This study was concerned with the isolation of novel bioactive compounds from endophytic fungi of the mexican yew tree (*Taxus globosa*). Endophytes are microbes which commonly live in the intercellular spaces of stems, petioles, roots, and leaves of plants causing no outward manifestation of their presence. The associations of these microbes to their hosts range from mutualistic, to symbiotic, to commensal.[21] The microbes may mimic the plant and make the same secondary metabolites as its host, or it may contribute by producing one or more compounds that may protect the plant (and thus itself) from attack by insects, fungi, bacteria, or other predators. It is probable that some of these

bioactive compounds may also have pharmaceutical applications.[22] Plant endophytes are a particularly unexplored niche of fungi, and of the work done, there is limited knowledge of the metabolites of these particular fungi. Together this makes endophytic fungi possibly one of the largest potential areas for discovery in the plant/microbe world.[23]

The choice of yew trees as a source of endophytic fungi was driven by the high cost and limited supply of taxol. The work done in the Stierle and Strobel laboratories to isolate a fungal source of taxol[24] resulted in a large collection of fungi which could also be examined for other bioactive metabolites.

Preliminary Results

Six fungi isolated from the mexican yew (labled as MA17, MC1, ME1, ME7, ME19, MF1) were chosen for this study. The fungi were purified and grown in 300 ml of sterilized medium containing 10.0 g sucrose, 1.0 g Bacto-Soytone, and 1 ml of a 1.0 M phosphate buffer (pH = 6.8) per liter. The cultures were incubated at room temperature without shaking for twenty-one days.

The mycelia were removed by filtration through eight layers of cheesecloth. The mycelia were then ground and extracted with 1:1 chloroform:methanol for the mycelial/organic (M/O) fraction and then with water for the mycelial/aqueous (M/H_2O) fraction. The filtrate medium was also extracted with three successive portions of chloroform and two portions of ethyl acetate. The organic extracts

were combined for the filtrate/organic (F/O) fraction and the remaining aqueous solution was lyophilized and labeled as the filtrate/aqueous (F/H_2O) fraction.

The crude extracts were subjected to a brine shrimp toxicity assay and to agar-diffusion assays to test for bioactivities (See Chapter 2 for details). The agar-diffusion assays were carried out on 0.5 mg of each extract dissolved in 20 µL of methanol. Positive results are recorded on a scale (+ to +++++) according to the completeness and size of the zone of inhibition. Negative results are recorded as a negative (-) and those with multiple negatives (-- and ---) were zones of apparent growth promotion. The brine shrimp toxicity assay was performed on 1.5 mg of extract in 60 µL of methanol per 3 mL of brine water for the organic extracts. The aqueous extracts were 1.5 to 5 mg of sample in 30 µL of water per 3 mL of brine water. Results are given as the number of dead brine shrimp at each time interval. The results of these bioassays are given in Tables 1.1 and 1.2.

There was very little activity in any of the aqueous fractions. However, several of the organic fractions were active in at least one of the bioassays. The severe brine shrimp activity of fraction MA17 F/O and the antifungal activity of the ME19 F/O fractions led to the isolation of sphaeric acid (Chapter 3) and epicorazine A (Chapter 6) respectively.

Extract	G. cand.	C. alb.	B. sub.	P. aerug.	E. coli
MA17 F/O	-	+	+++	++++	+++
MA17 M/O	-	-	+	-	-
MA17 F/H_2O	-	-	-	-	-
MA17 M/H_2O	-	-	-	-	-
MC1 F/O	-	+	+	-	-
MC1 M/O	+	++	+	-	-
MC1 F/H_2O	-	-	-	-	-
MC1 M/H_2O	+	---	-	-	-
ME1 F/O	-	-	++	-	-
ME1 M/O	-	-	+	-	-
ME1 F/H_2O	-	---	-	-	-
ME1 M/H_2O	+	-	+	-	-
ME7 F/O	+	+	++++	-	-
ME7 M/O	+	+	+	-	-
ME7 F/H_2O	-	--	-	-	-
ME7 M/H_2O	+	-	+	-	-
ME19 F/O	+++++	+++++	+++++	-	-
ME19 M/O	++	++	++	-	-
ME19 F/H_2O	-	+	-	-	-
ME19 M/H_2O	-	+	+	-	-
MF1 F/O	-	+	++++	-	-
MF1 M/O	+	+	+	-	-
MF1 F/H_2O	-	-	-	-	-
MF1 M/H_2O	-	-	+	-	-

Table 1.1 Antibiotic bioassays of crude extracts

Extract	t=0h	t=1h	t=3h	t=6h	t=12h	t=24h	total
MA17 F/O	13	26	45	-	-	-	45
MA17 M/O	0	0	0	0	0	0	44
MA17 F/H_2O	0	0	0	0	1	2	15
MA17 M/H_2O	0	0	0	0	0	0	23
MC1 F/O	0	0	1	11	29	32	32
MC1 M/O	0	0	0	0	1	2	22
MC1 F/H_2O	0	0	0	0	2	2	25
MC1 M/H_2O	0	0	0	0	0	1	16
ME1 F/O	0	0	1	1	1	4	42
ME1 M/O	0	0	0	0	0	13	42
ME1 F/H_2O	0	0	0	0	0	1	23
ME1 M/H_2O	0	0	0	0	5	5	11
ME7 F/O	0	0	2	2	3	14	30
ME7 M/O	0	0	0	0	0	1	37
ME7 F/H_2O	0	0	0	0	0	0	25
ME7 M/H_2O	0	0	0	0	0	1	20
ME19 F/O	0	0	0	0	2	14	24
ME19 M/O	0	0	0	0	0	0	27
ME19 F/H_2O	0	0	0	0	2	2	22
ME19 M/H_2O	0	0	0	0	0	3	22
MF1 F/O	0	0	0	0	4	18	22
MF1 M/O	2	0	0	1	2	2	48
MF1 F/H_2O	0	0	0	0	5	4	34
MF1 M/H_2O	0	0	0	0	0	10	25

Table 1.2 Brine shrimp bioassays of crude extracts

Fungal Identification

The identification of the fungi involved in this study was performed by Dr. Gene Ford. ME19 was identified as an *Epicoccum* sp. based on its spore characteristics. However, the identification of MA17 was not so straightforward. By the time Dr. Ford examined the fungus, it had lost its ability to produce spores in culture under the same conditions that it had when originally isolated. His identification was then based on the initial observations of spores produced in early cultures and their documentation by photomicrographs.

Several authorities on mycological taxonomy examined cultures of this isolate. None of them were able to make a positive identification because of the inability to obtain adequate sporulation of the fungus. However, the fungus produces sterile fruiting structures (dark colored pycnidia with curled setae adorning the area around the ostiole) on many media. All the authorities agreed that the fungus belongs to the *Sphaeropsidales*. Brian C. Sutton believed the fungus is possibly a *Phyllosticta*, but without spores to examine, admitted this is an educated guess based only on hyphal and cultural appearance. R. A. Samson (Centraalbureau voor Schimmelcultures) considered it to possibly be a *Diplodia*, even though he did not observe any two-celled spores in culture. Likewise, Jeffery Stone at Oregon State University cultured the fungus and got a microconidial stage (possibly *Leptodothiorella*) and a pycnidial stage which produced dark single-celled spores which he speculated might be an immature

Diplodia stage. However, he did not observe any two-celled spores. A fourth mycologist from the University of Toronto, David Mallock, speculated that the fungus is *Chaetodiplodia* based on the setae found on the pycnidia. However, this ID also requires the spores to be two-celled.

In light of the inability of these experts to agree on an identification and using our own observations on fruiting body and spore formation, Dr. Ford believes this fungus to be a *Sphaeriopsis* sp. The reasons for this are as follows:

1) Only dark colored, single-celled pycnidiospores were observed, which rules out *Diplodia* which has two-celled spores.

2) Spore measurements showed their size to average 27.1 µm X 14.2 µm, which is slightly smaller than that reported for other members of this genus (30-45 µm X 10-22 µm).

3) No microconidial production was ever observed in our cultures.

Moreover, the setae adorning the pycnidia are produced under all cultural conditions (including culture on sterilized *Taxus* leaves), thus providing a constant character to be used in classifying this fungus. The small spore size and slightly coiled setae with their ornamentations could provide justification for the establishment of a new species.

Figure 1.1 shows the photomicrographs of the *Spaeriopsis* sp. From upper left to lower right the photos are as follows:

1) UL: Setae of pycnidium on a yew twig from above (Approximately X75).

2) UR: Pycnidium emerging from a yew twig (X200).

3) CL: Setae and pycnidium on a yew twig from the side (X400).

4) CR: Ornamentations on setae (X3000).

5) LL: Cross-section of seta and ornamentations (X14,500).

6) LR: Pycnidiospores (X170).

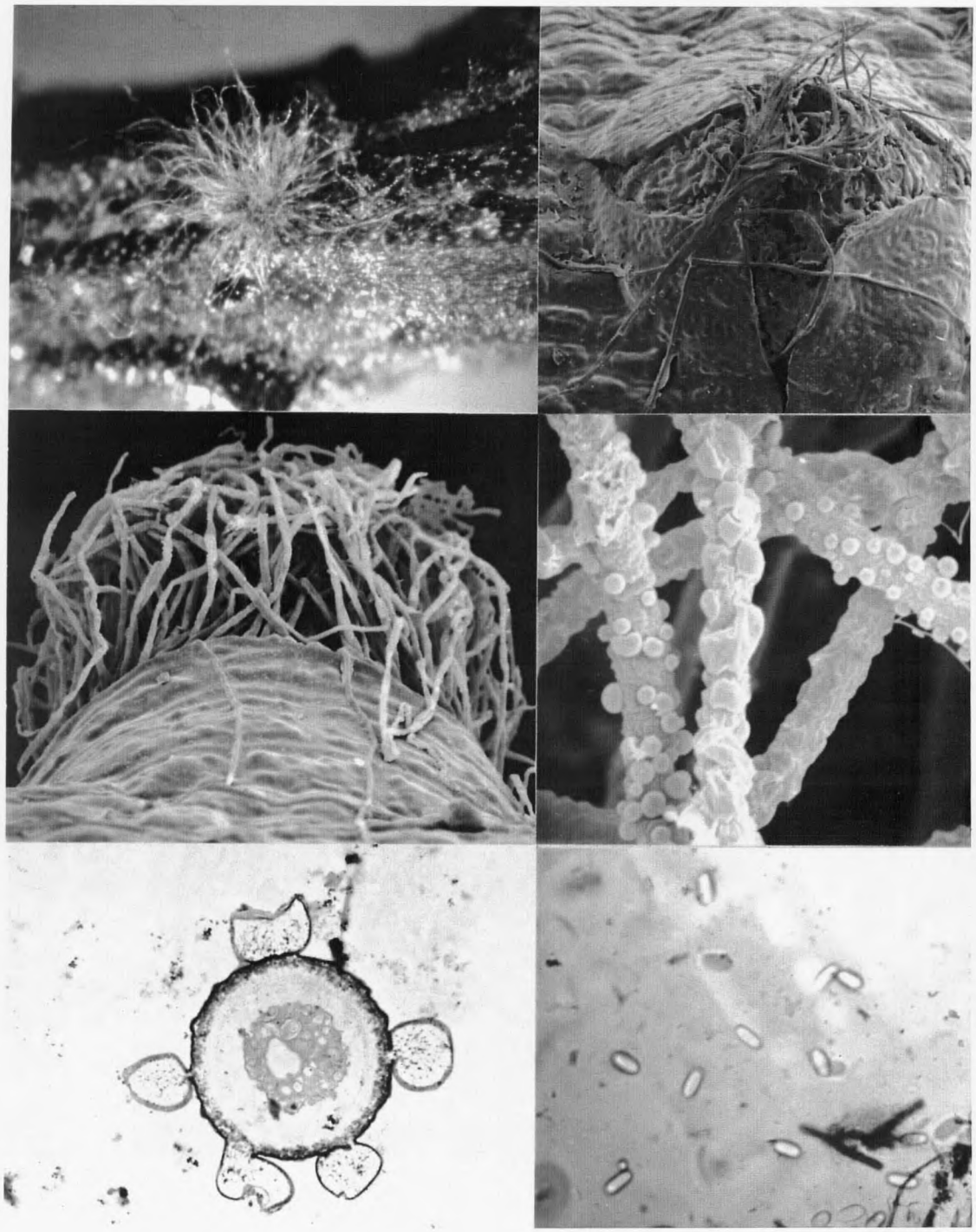

Figure 1.1 Photomicrographs of *Sphaeriopsis* sp.

Chapter 2

GENERAL EXPERIMENTAL METHODS

Throughout the scope of this work, there were many experimental methods which remained constant. This chapter covers the experimental portions for these processes. These are involved throughout the work from the fungal isolation, maintenance, and culturing, to the isolation and structure elucidation of the natural products, and to the determination of the biological activities of the compounds.

Fungal Isolation

The initial fungal isolation was performed by Dr. Bret Niedens. Twig samples of *Taxus globosus*, mexican yew, were surface sterilized with 95% ethanol. After evaporation of the ethanol in a sterile laminar flow hood, the outer bark of the twigs were removed. Small (~1 cm) pieces of inner bark (phloem-cambium and xylem tissues) were removed and placed on water agar plates. After a period of initial growth, hyphal tip transfers of the developing fungi were grown on potato dextrose agar and visually checked for purity.

Fungal Maintenance and Culturing

Microbial samples were maintained on a variety of agars, including Tryptic Soy Agar, Potato Dextrose Agar, M-1-D agar. Agars were prepared from Difco Microbiological agars, or from the corresponding Difco broths and Difco Bacto agar, except M-1-D (shown below). Fungi isolated from yew trees were maintained on the above agars containing 1% yew broth (discussed below).

Fungal culturing was carried out in a variety of synthetic media labled R-1, R-2, medium A, medium B, and medium C. Medium R-1 was the standard medium used in this study and medium R-2 was a high sugar/high nutrient version of medium R-1. Media A, B, and C were a series of trapping media used to limit the amounts of certain nutrients during culturing. The culturing was done in four liter and two liter erlenmeyer flasks, and one liter roux flasks. The volume of medium in each flask was generally chosen to give the largest surface area for growth. Fungi were grown for twenty-one days in still culture, with occasional swirling in some instances.

Yew Broth

Five grams of yew needles and small stems were placed in a beaker with 500 ml of water. The water was boiled for 5 minutes and then allowed to simmer for one hour without heating. The broth was passed through cheesecloth to remove the yew debris and the broth was frozen in ten milliliter portions.

M-1-D Agar

Major salts: $Ca(NO_3)_2$ - (0.28 g/L), KNO_3 - (0.08 g/L), KCl - (0.06 g/L); Minor salts: $FeCl_3 \cdot 6H_2O$ - (2.0 mg/L), $MnSO_4$ - (5.0 mg/L), $ZnSO_4 \cdot 7H_2O$ - (2.5 mg/L), H_3BO_3 - (1.4 mg/L), KI - (0.7 mg/L); $MgSO_4$ anhyd. - (0.36 g/L), $NaH_2PO_4 \cdot H_2O$ - (0.02 g/L), ammonium tartrate - (5.0 g/L), sucrose - (30 g/L), yeast extract (Difco) (0.25 g/L), agar (15 g/L).

R-1 Medium

Bacto soytone (Difco) - (1.0 g/L), sucrose - (10 g/L), 1.0 M $KHPO_4$ buffer (1.0 mL/L).

R-2 Medium

Bacto soytone (Difco) - (5.0 g/L), sucrose - (60 g/L), yeast extract (Difco) - (1.0 g/L), 1.0 M $KHPO_4$ buffer (1.0 mL/L).

Medium A

Bacto soytone (Difco) - (10 g/L), glucose - (40 g/L), $Mg_3(PO_4)_2 \cdot 12H_2O$ - (10 g/L).

Medium B

Bacto soytone (Difco) - (10 g/L), glucose - (40 g/L), $MgCO_3$ - (10 g/L).

Medium C

Bacto soytone (Difco) - (10 g/L), glucose - (40 g/L), $MgSO_4 \cdot 7H_2O$ - (20 g/L).

Extraction and Purifications

All initial mycelia and media extractions were conducted with Fisher Chemical HPLC grade solvents, EM Science HPLC grade solvents or Fisher Chemical ACS grade solvents. Water used for extractions was distilled water from a Wheaton Autostill 1.5 water still.

Low pressure chromatography was performed with various solid supports including Lipophilic Sephadex LH-20 (25-100 µm beads), Toyopearl HW-40F (45 µm beads), BioRad Chelex 100 (50-100 mesh), and J.T. Baker silical gel 40 µm flash chromatography packing. Solvents used were Fisher Chemical HPLC grade solvents and EM Science HPLC grade solvents. Water was distilled with a Wheaton Autostill 1.5 water still. Fractions were collected on a Gilson FC203B fraction collector, and fractions were determined by use of a Gilson 115 variable wavelength UV/VIS detector.

The HPLC system consisted of Waters 510 HPLC pumps, a Waters model 660 Solvent Programmer, a Waters model U6K Injector, and a Waters model 440 Absorbance Detector. Columns used were purchased from Rainin including:

Analytical:

Dynamax 60Å silica column, 4.6 mm ID X 25 cm L, 8 µm packing.

Microsorb silica column, 4.6 mm ID X 25 cm L, 5 µm packing.

Semi-preparative:

Dynamax 60Å silica column, 10 mm ID X 25 cm L, 8 µm packing.

Dynamax 60Å octadecyl column, 10 mm ID X 25 cm L, 8 µm packing.

Preparative:

Dynamax 60Å octadecyl column, 21.4 mm ID X 25 cm L, 8 µm packing.

All columns were protected by Rainin guard columns (5 cm L) of matching diameter and packing material. Solvents used were Fisher Chemical HPLC grade solvents and EM Science HPLC grade solvents. Water was distiilled by a Wheaton Autostill 1.5 water still. All solvents were filtered and degassed with Kontes Brand Ultra-Ware HPLC Resevoir systems through Gelman 5 µm PTFE membrane filters.

Bioassays

In order to establish the presence of bioactive compounds, to follow them through the isolation procedure, and as a final characterization of the purified compounds, bioassay screening methods were used. The screening methods included simple agar-diffusion assays for the antibacterial and antifungal activities, and brine shrimp toxicity bioassays for antitumor bioactivity. Final characterization assays included a paper disc diffusion assay, a mouse thymocyte proliferation assay, an inhibitory concentration against breast adenocarcinoma BT-20 assay, a minimum inhibitory concentration spot test, and a brine shrimp toxicity assay.

Agar-diffusion Assay

In this assay, the fractions to be tested were dissolved in a small amount of solvent and then spotted (10 µL) on an agar medium [Difco Antibiotic Medium 1 (Penassay Seed Agar) for bacteria, and Difco Potato Dextrose Agar for fungi]. The solvent was allowed to evaporate and then the test microbe was inoculated on the plate. The inoculation was accomplished by spraying the plate with an aqueous suspension of the microbe. A positive assay was inhibition of the growth of the microbe in the area where the sample was applied. This method was used to test for antifungal compounds against *Geotrichum candidum* and *Candida albicans* and antibacterial compounds against *Bacillus subtilis*, *Pseudomonas aeruginosa* and *Escherichia coli*.

Brine Shrimp Bioassay

This assay was established as a general bioassay for a broad spectrum of pharmacological activities.[25] It is a convenient tool for isolating antitumor agents. Ferrigni and McLaughlin[26] used this assay to follow activity through fractionations in the isolation of piceatannol, an antileukemic compound, from the seeds of *Euphorbia lagascae*.

In this assay, the sample was dissolved in a small amount of solvent and added (30 µL of methanol) to a test vial of artificial sea water (3.0 ml). Approximately 20 brine shrimp, *Artemia salina*, were added to the vial. The brine shrimp were observed periodically over a twenty-four hour period and the number of dead brine shrimp in each vial were recorded. A positive assay was

the death of all or most of the brine shrimp by the end of the twenty-four hour period.

Paper Disc Diffusion Assay

This assay was a variation of the agar-diffusion assay[27] and was performed in the Stierle's laboratory at Montana Tech in Butte. The difference was the method of application of the sample. A known amount of sample (100 µg, 50µg, or 10 µg) dissolved in solvent was applied to a Difco Bacto Sterile Blank concentration disc, and the solvent was allowed to evaporate. The paper disc wais then placed on the agar and the test microbe was applied. The microbes tested against in this assay were *B. subtillis*, *Staphylococcus aureus*, *E. coli*, *P. aeruginosa*, *Vibrio harveyii*, *C. albicans*, *G. candidum*, *Aspergillus niger*, and *Fusarium oxysporum*.

Mouse Thymocyte Proliferation Assay

The interleukins are a group of glycoproteins which are involved in the regulation of the immune system. Interleukin-1 (IL-1) plays a central role in T-cell activation and has been found to be involved in a number of aspects of inflammation.[28] This assay was used as a general screen for agents that affect IL-1 action.

This assay was performed by Pharmagenesis Pharmaceuticals in Palo Alto, CA and the inhibition of IL-1 mediated thymocyte proliferation was reported.

The procedures followed were the standard, published procedures reported in Laboratory Methods in Immunology.[29]

Minimum Inhibitory Concentration (MIC) Against Breast Adenocarcinoma BT-20

This assay was performed by Cytoclonal Pharmaceuticals, Inc. in Dallas, Texas. The human breast cell cancer lines were exposed to serial dilutions of each derivative. After three days of exposure, the cells were stained with neutral red and the absorbance was measured at 540 nanometers. Samples were dissolved in either methanol or dimethylsulfoxide at negligible levels. The results were reported as inhibitory concentration (IC_{50}) values.

Minimum Inhibitory Concentration (MIC) Spot Test

Extracts were dissolved in methanol or chloroform to final concentrations of 10 µg/µL. Serial dilutions of each sample were made giving final test concentrations of 10, 5 and 2.5 µg/µL. Five microliters of each solution were spotted onto a half-strength YM agar plate (10.5 g/L YM broth (Difco), 15 g/L agar), and allowed to dry. An agar solution, containing *C. albicans,* was prepared to have an $O.D._{590}$ of 0.3. Three millilters of this agar was overlayed on the spotted agar plates and allowed to harden. The plates were incubated for 24 hours at 37 C and observed to determine the MIC as the last dilution where activity was observable.

Organisms for Antibiotic Assays

The microorganisms chosen for the antibiotic assays were chosen to give a broad basis to determine activity. These included the fungi and bacteria (Gram-positive and Gram-negative) indentified below.

Geotrichum Candidum: A member of Fungi Imperfecti that is ubiquitous in soil and dairy products, it is sometimes pathogenic in human respiratory and gastrointestinal tracts.[30]

Candida albicans: A yeast-like fungus, that is found in human and animal digestive tracts which can invade other tissues under certain conditions.[31] Invasive candidiasis is the most common fungal infection in patients with HIV infection, and is associated with increased mortality in bone marrow transplant recipients.[32]

Bacillus subtilis: It is a Gram-positive bacterium that is one of the most common non-pathogenic aerobic spore formers. It is related to *B. anthracis* which is the agent responsible for anthrax in cattle, sheep, and other agriculturally important animals.[33]

Pseudomonas aeruginosa: This is a Gram-negative bacterium and is the only Pseudomonas species that is pathogenic for man and animals.[34] It remains a problem pathogen, becoming resistant to virtually all the clinical antibacterial agents, and is a major challenge in the field of antibiotics.[35]

Escherichia coli: *E. coli*, a Gram-negative bacterium, is the predominant organism in the intestinal canal of man and animals. It can become pathogenic

and may invade the appendix, gall-bladder, peritoneal cavity, kidneys, and the urinary bladder.[36]

Staphylococcus aureus: A Gram-positive, pathogenic, bacterium which man and animals live with from birth until death, it only becomes infectious when their susceptibility is appreciably affected.[37] Its resistance has increased recently and currently vancomycin is the only clinical antibiotic that provides reliable activity against multiply resistant strains.[38]

Vibrio harveyii: This is a Gram-negative marine bacterium which is the primary colonizer in marine fouling. It is related to disease causing Vibrio including *V. choleræ* responsible for cholera.[39]

Aspergillus niger: Aspergillus is a pathogenic filamentous fungus which has a propensity for invasion of blood vessels.[40]

Fusarium oxysporum: The Fusarium are members of the Fungi Imperfecti which include saprophytes and many plant parasites.[41] It is emerging as a human pathogen in immunocompromised patients and often does not repsond to conventional doses of amphotericin B.[42]

Instrumentation for Structure Elucidation

Ultraviolet/Visible Spectrometer: Beckman DU-50 UV/VIS Spectrophotometer.

Polarimeter: Optical rotations were collected on a Perkin-Elmer model 241 MC polarimeter.

Infrared Spectrometer: IR spectra were collected on a Perkin-Elmer model 1600 FTIR.

Mass Spectrometry: Mass spectra were recorded on a VG 10E-HF Mass Spectrometer or a TRIO-2 Electrospray Mass Spectrometer.

TMS derivatives were prepared by reacting the sample with BSA [*N,O*-Bis(trimethylsilyl)acetamide].

Nuclear Magnetic Resonance: NMR spectra were recorded on a Bruker AC300 spectrometer, a Bruker DPX300 spectrometer, a Bruker DRX250 spectrometer, or a Bruker DRX500 spectrometer. Carbon assignments (methyl, methylene, methine, quaternary) were determined via DEPT 90 and DEPT 135 experiments.

Chapter 3

SPHAERIC ACID

One of the most interesting activities from the preliminary bioassays of the crude extracts was the strong activity of the MA17 F/O fraction in the brine shrimp toxicity bioassay (Table 1.2). Activity-guided fractionation of this extract led to the isolation of a novel compound, sphaeric acid (Figure 3.1).

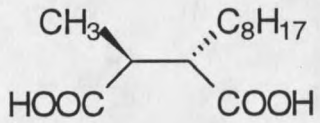

Figure 3.1 Sphaeric acid
(Absolute Stereochemistry unknown)

Sphaeric acid is a member of a class of alkylated succinic acid derivatives, many of which contain more oxidized functional groups than just the two carboxylic acids. Most of these succinic acid derivatives were isolated in non-bioassay guided searches for new compounds. However, there were a series of mono and dialkyl succinic acids sythesized in a search for antitubercular compounds.[43,44]

Roccellic acid and pedicellic acid (Figure 3.2) are the members of this class most similar to sphaeric acid, being 2-alkyl-3-methyl succinic acids. In addition

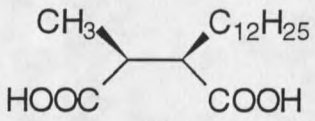

roccellic acid

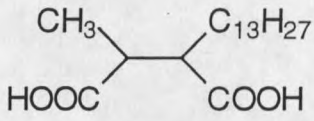

pedicellic acid

Figure 3.2 Roccellic and pedicellic acids

to having a longer alkyl chain, the two alkyl groups are cis in roccellic acid[45] when written as a succinic acid derivative, but in a trans configuration in sphaeric acid. Pedicellic acid is the only example of this skeleton found in higher plants[46], while roccellic acid and the other more oxidized products[47] (Figure 3.3) have been isolated from lichens.

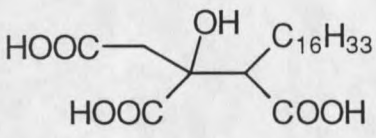

agaricic acid

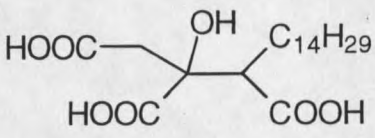

caperatic acid

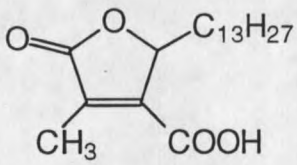

lichesteric acid

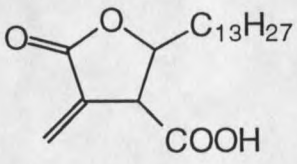

protolichesteric acid

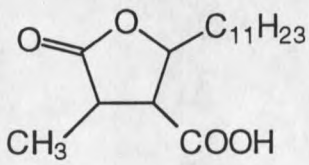

nephrosteranic acid

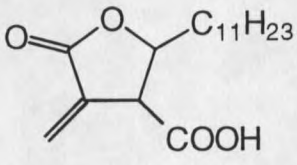

nephrosterinic acid

Figure 3.3 Succinic acid based natural products

Sphaeric acid was isolated because of its activity in the brine shrimp toxicity assay. There was some concern that the brine shrimp toxicity may have been due to the acidity of sphaeric acid. However, the concentrations tested only lowered the pH to approximately 5.6, while a pH as low as 4.0 seemed to show no toxicity to the brine shrimp over the twenty-four hours of testing. The purified diacid was also tested for other activities and gave a positive result in a mouse thymocyte proliferation assay without being cytotoxic at the concentrations tested. This is a general screening assay for agents that affect interleukin-1 (IL-1) action, which plays a central role in T-cell activation of the immune system.[48]

Isolation and Structure Elucidation of Sphaeric Acid

The *Sphaeriopsis* sp. isolated from the inner bark of the mexican yew tree, *Taxus globosa*, was grown in still culture in R-1 media for 21 days. The mycelia were removed by filtration through eight layers of cheesecloth and the filtrate was extracted with methylene chloride. The extract was chromatographed on Sephadex LH-20 and eluted with 1:1 $CHCl_3$:MeOH. The active fractions were subjected to reverse-phase HPLC and eluted with a linear gradient from 70% methanol in water to 100% methanol. The active fraction was submitted to a final separation on a Toyopearl TSK gel and eluted with 2:1 MeOH:H_2O, and pure sphaeric acid was collected.

The high resolution CIMS gave a molecular formula of $C_{19}H_{41}O_4Si_2$ for the protonated TMS derivative of sphaeric acid. Replacing the two TMS groups (C_3H_9Si) with protons gave a molecular formula of $C_{13}H_{24}O_4$. This molecular formula allowed for two sites of unsaturation. The IR signal at 1707 cm^{-1} and the carbon NMR signals at 182.3 and 182.1 ppm suggested the presence of

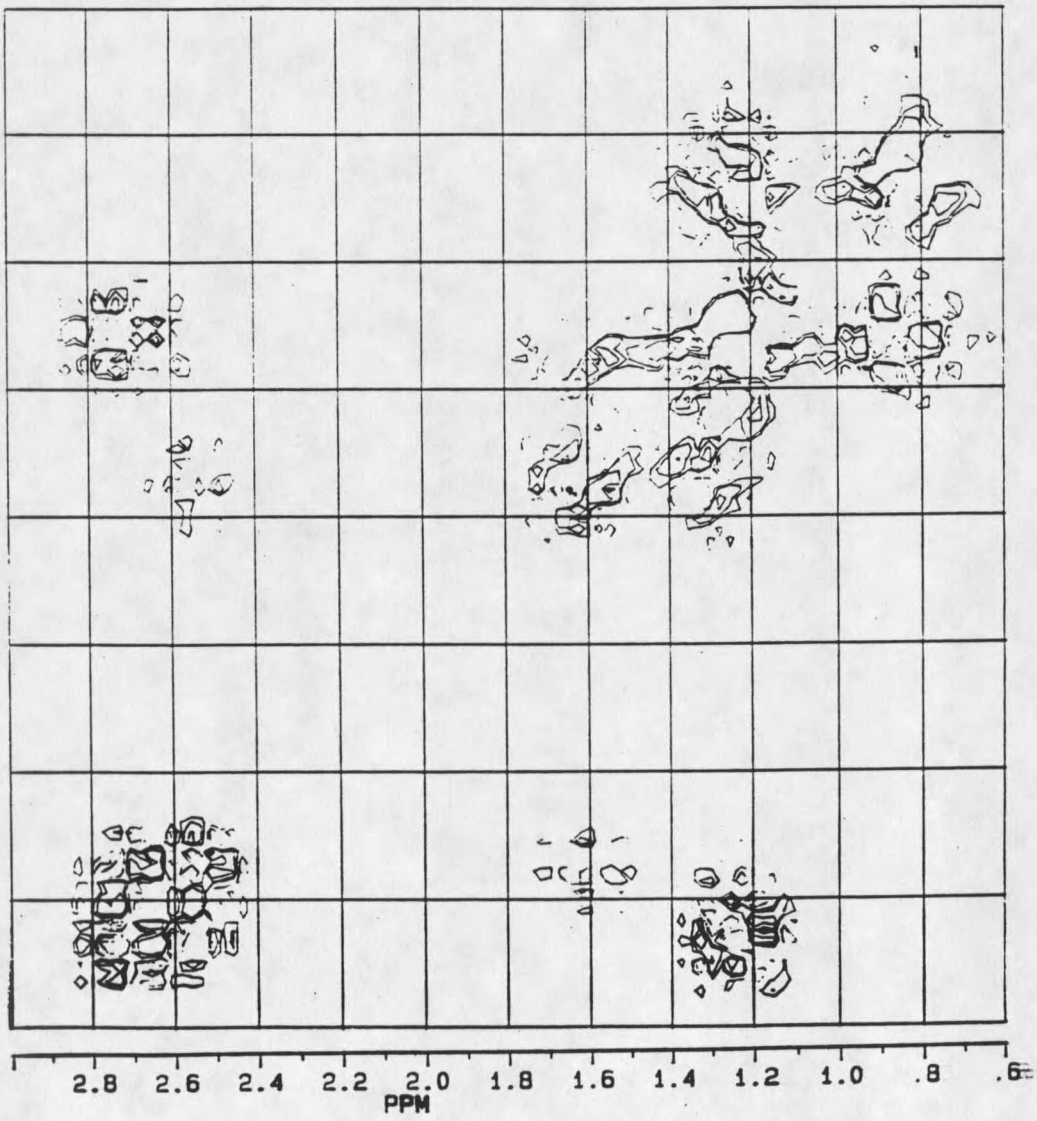

Figure 3.4 COSY of sphaeric acid

two carboxylic acid groups. The two D_2O exchangeable protons at 11.5 ppm in the proton NMR supported the presence of two carboxylic acid groups. This accounted for the two sites of unsaturation, so the rest of the molecule must be saturated.

The carbon NMR data indicated that there were two methyl groups and two methines in the molecule, and the remainder of the signals were methylenes. This, as well as the large proton signal at 1.2 ppm, suggested the presence of a long alkyl chain. The triplet at 0.85 ppm, which integrated to three protons, was typical for a terminal methyl of an alkyl chain.[49] The methine protons were the lowest field protons which each integrated to a single proton. The additional methyl group was included in the signal at 1.2 ppm which accounted for its integration to an odd number of protons (15).

The COSY spectrum of sphaeric acid (Figure 3.4) shows that the two methines at 2.7 ppm and 2.5 ppm coupled to each other. Additionally, the methine at 2.5 ppm coupled to the methylene protons at 1.6 ppm, and the methine at 2.7 ppm coupled to the signal at 1.2 ppm. Since the methine at 2.7 ppm is a doublet of quartets, it must be coupled to the methyl group within the 1.2 ppm signal as well as the other methine. The methine at 2.5 ppm being a doublet of triplets also supported it being coupled to the methylene at 1.6 ppm and the other methine. This gave the basic structure shown in Figure 3.5.

The remaining two sites on the methines must then be the two carboxylic acid groups. This was supported by the absence of other proton signals downfield

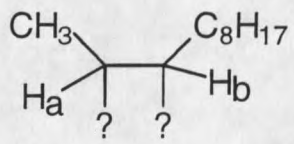

Figure 3.5 Partial Structure of Sphaeric Acid

enough to be adjacent to the carboxylic acid groups, which typically come lower than 2.0 ppm.[50] This gave the final structure for sphaeric acid without stereochemistry as shown in Figure 3.6.

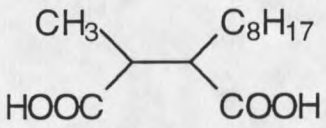

Figure 3.6 Sphaeric Acid (No Stereochemistry)

The relative stereochemistry of the two chiral carbons is based on a comparison to the pair of synthetic lactone derivatives shown in Figure 3.7 (structure elucidation below). Sphaeric acid was reduced with lithium aluminum

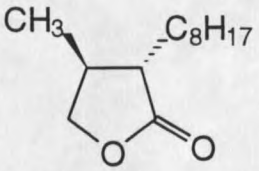

Lactone A

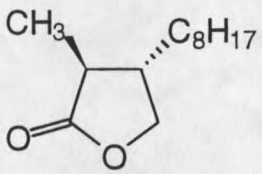

Lactone B

Figure 3.7 Lactone derivatives of sphaeric acid
(Absolute stereochemistry unknown)

hydride to produce the dialcohol. Upon oxidation of the dialcohol with pyridinium chlorochromate (PCC), the lactones A and B were recovered instead of the expected dialdehyde.

The relative stereochemistry was assigned by comparison of the lactones to the known compounds (+)-pilocarpine and (+)-isopilocarpine (Figure 3.8). The chemical shifts of the methylene protons adjacent to the oxygen in the lactone ring were particularly diagnostic. The two isomers, pilocarpine and isopilocarpine, have different chemical shifts for the two protons of the methylene groups (4.05 and 4.15 for pilocarpine and 3.89 and 4.39 for isopilocarpine[51]). The trans stereochemistry was chosen because of the similarity of the methylene protons of the synthesized lactones (4.4/4.3 and 3.8/3.7) to the isopilocarpine signals giving the relative stereochemistry shown in Figure 3.1.

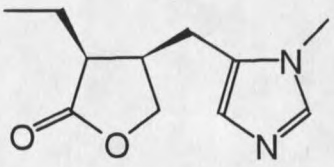

(+)-pilocarpine

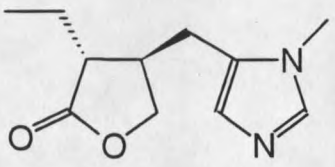

(+)-isopilocarpine

Figure 3.8 Pilocarpine and isopilocarpine

Lactone Structure Elucidation

The high resolution GC/EIMS was able to resolve the two lactones, A and B, both of which gave a molecular formula of $C_{13}H_{24}O_2$. The molecular formula

allowed for two sites of unsaturation, but an inspection of the proton NMR shows that the product of the oxidation was not the expected dialdehyde. The two groups of proton signals at 4.3-4.4 ppm and 3.7-3.8 ppm were too low to be the methine protons of the expected dialdehyde (figure 3.9). Additionally, there was no evidence of the aldehyde protons around 9.5-10.0 ppm.[52]

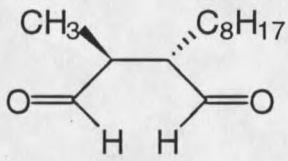

Figure 3.9 Expected dialdehyde of sphaeric acid

The carbon NMR signals at 180.2 and 179.8 ppm suggested the presence of an acid or ester functional group. The ester functionality was also supported by the presence of the oxygen bearing methylenes at 73.0 and 72.1 ppm. Oxidation of one of the hydroxyls followed by cyclization led to the two γ-lactones. The IR peak at 1777 cm^{-1} was supportive of this since the carbonyl of γ-valerolactone[53] (Figure 3.10) absorbs at 1770 cm^{-1}.

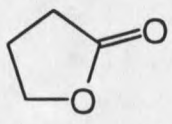

Figure 3.10 γ-Valerolactone

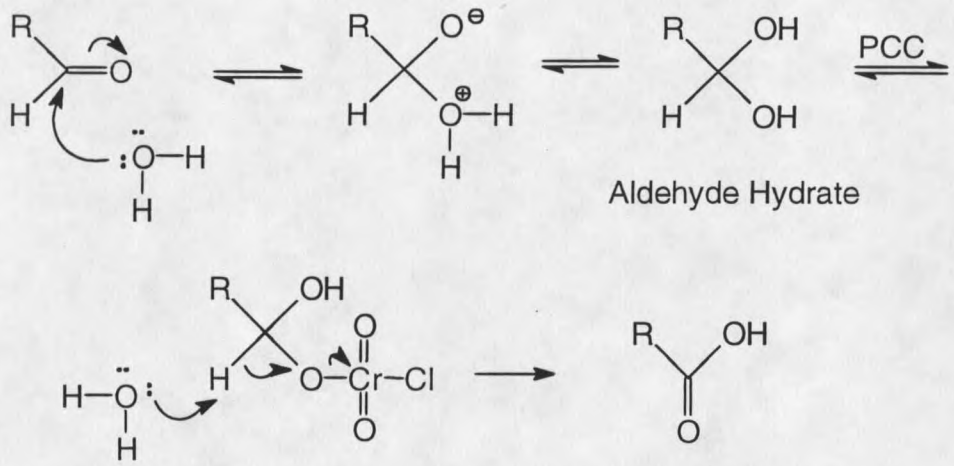

Figure 3.11 Aqueous chromate oxidation to a carboxylic acid

The synthesis of the lactones instead of the dialdehyde can be explained through the formation of an intermediate similar to the aldehyde hydrate formed in an aqueous chromate oxidation of a primary alcohol to a carboxylic acid[54] (Figure 3.11). Instead of attack by the water molecule which leads to the

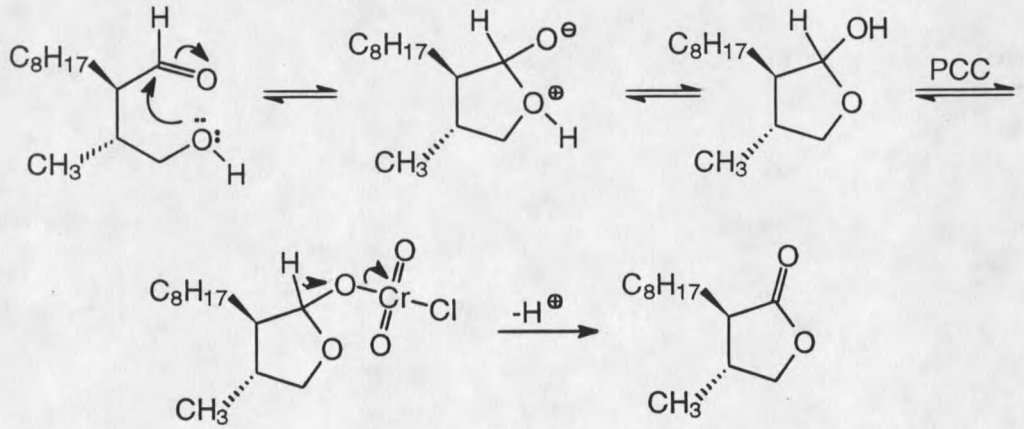

Figure 3.12 Formation of lactones

formation of a carboxylic acid, the neighboring hydroxyl group attacks leading to the formation of the lactone (Figure 3.12).

Mass Spectral and NMR Assignments of Lactones

The two lactones had different retention times in the GC/MS allowing for the identification of each one. As can be seen in Figures 3.16 and 3.17, the two isomers fragment differently. The first one to elute, lactone A, had a base peak of 100, with large peaks at 85 and 113. Lactone B, on the other hand, had a base peak of 55, with large peaks at 70 and 99. The identification of the lactones was based on the base peak of lactone A having a mass of 100. This mass is produced via a γ-H rearrangement to a carbonyl with β-cleavage, or McLafferty rearrangement, shown in Figure 3.13. This is a common rearrangement for carbonyl compounds with a γ proton that goes through a sterically favorable six-membered ring transition state.[55] Lactone B, with the

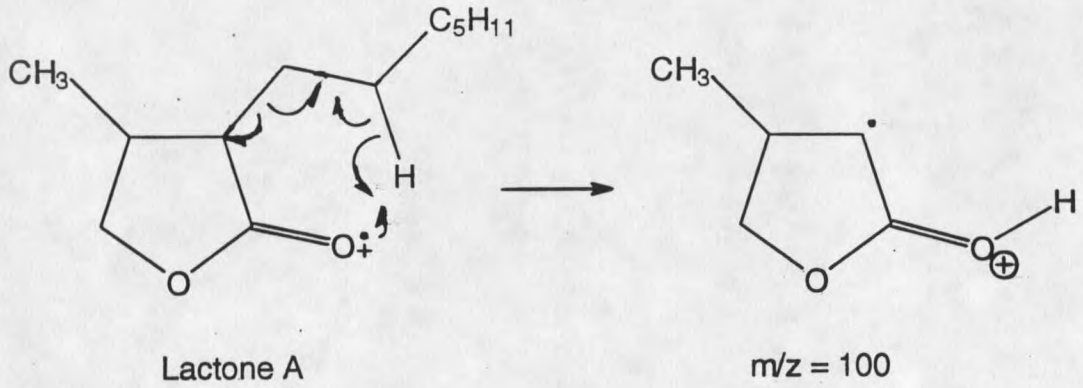

Figure 3.13 Fragmentation of Lactone A

carbonyl on the other side of the ring, cannot undergo this rearrangement, and must fragment by other methods, leading to the smaller mass fragments.

The proton assignments of the protons on the lactone ring can be made using the COSY of the lactones (Figure 3.14). The proton at 2.3 ppm correlated to the methyl signal at 1.1 ppm, as well as the 4.2 ppm/3.7 ppm pair for the methylene adjacent to the oxygen of the ester. This combination can only occur with lactone A. This proton also coupled to the proton at 2.1 ppm. On

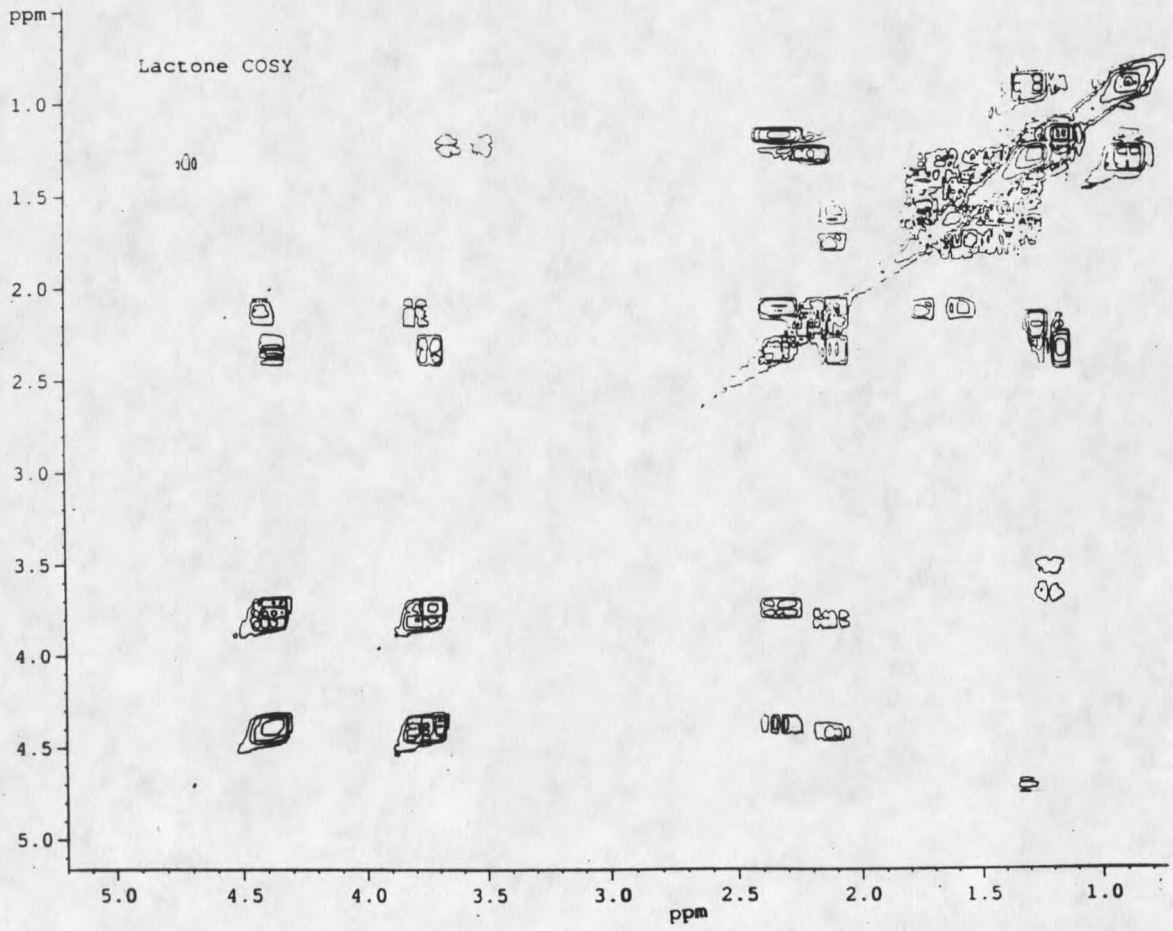

Figure 3.14 COSY of lactones

the other hand, the methyl signal of lactone B at 1.2 ppm coupled to the methine signal at 2.2 ppm. The methylene protons at 4.4 ppm and 3.8 ppm correlated to the methine signal at 2.1 ppm which also coupled to the other methine. This gave the resulting assignments shown in Figure 3.15. This allowed for the determination of the relative amounts of the lactones produced. Using the integration figures of the methyene protons at 3.8 ppm and 3.7 ppm, it appeared that the ratio was approximately 55:45 for the two lactones (A:B).

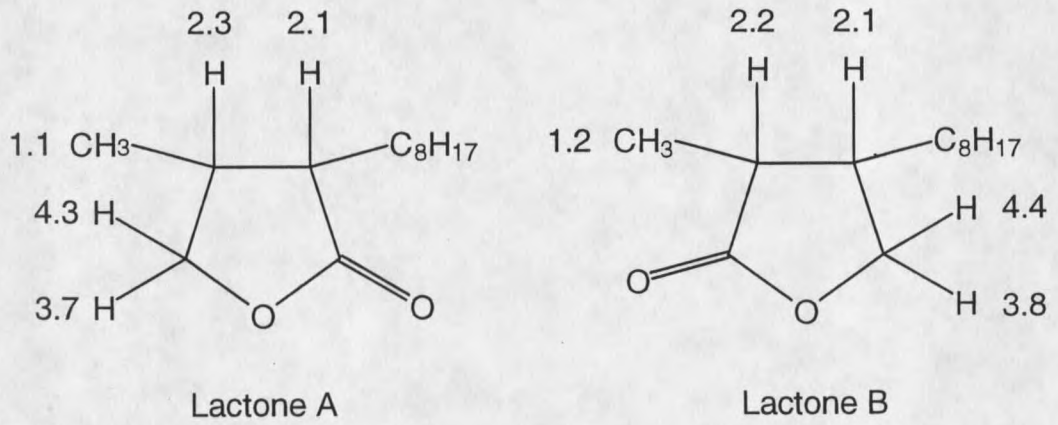

Figure 3.15 Proton assignments of lactones

Experimental

Culture Conditions

The *Sphaeriopsis* sp., labled as MA-17, was maintained on M-1-D agar containing 1% yew broth. MA-17 was grown in still culture in two liter erlenmeyer flasks and 1000 ml roux flasks in R-1 media containing 1% yew

broth for 21 days. Since MA-17 grew on the surface of the culture liquid the amount of liguid used in each flask was chosen to give the largest surface area for growth.

Extraction and Isolation

The fungal mycelia were removed by filtration through eight layers of cheesecloth, and the filtrate was extracted once with 400 mL of methylene chloride. The filtrate was acidified to pH = 1 and extracted with two additional 400 mL portions of methylene chloride. The extracts were combined and evaporated to dryness on a rotoevaporator (23.5 mg/L). The extracts were chromatographed on a Sephadex LH-20 column (2.8 cm X 110 cm), and eluted with 1:1 $CHCl_3$:MeOH. Nine total fractions were collected and isolation of the active compound was carried out by activity-guided fractionation using a brine shrimp toxicity bioassay. Fractions 4 and 5 (19.5 mg), were then chromatographed by reverse phase HPLC on a preparative Rainin Dynamax 60-Å C18 column by gradient elution using a linear gradient from 70% methanol in water to 100% methanol, followed by a methylene chloride wash. Four fractions were collected, with fraction 3 (11.6 mg) exhibiting activity. This fraction was submitted to a final separation on a Toyopearl TSK gel HW-40F column (2.8 cm X 40 cm) and eluted with 2:1 MeOH:H_2O. Sixteen fractions were collected, with fraction 2 giving pure sphaeric acid (7.1 mg).

Reduction to Diol

Sphaeric acid (11 mg, 0.046 mmole) in anhydrous ether (0.5 ml) was added dropwise through the condenser to a solution of lithium aluminum hydride (15 mg, 0.39 mmole) in anhydrous ether (0.5 ml). The solution was refluxed for one hour and cooled. The excess hydride was decomposed by adding 1 ml "wet" ether and refluxing for an additional 15 min. "Wet" ether was prepared by mixing equal parts of ether and water and retaining the upper organic layer. Sulfuric acid (~10 % aq, 4 mL) was added to dissolve the aluminum complex, and the aqueous solution was extracted with three 5 ml portions of chloroform. The combined extracts were dried over anhydrous magnesium sulfate and evaporated to give pure diol (10 mg, 0.046 mmole).

Oxidation to Lactones

Diol (10 mg, 0.046 mmole) in methylene chloride (1.0 ml) was added to pyridinium chlorochromate (22 mg, 0.10 mmole) in methylene chloride (1.0 ml) and the solution stirred for 3 hours. The chromium reagent was removed on a flash silica column (1 cm X 2 cm) and eluted with methylene chloride. The lactones (5 mg, 0.024 mmole) was recovered by overnight evaporation of the methylene chloride.

Physical/Chemical Data for Sphaeric Acid

Light yellow oil; $[\alpha]^{25}D$ +7 (23 mg/ml, CH_3OH); UV (CH_3CN) λ_{max} (ε) 205 (159); IR υ_{max} (cm^{-1}) (neat) 2919 br, 1707, 1460, 1413, 1278, 1225, 931, 720; HRCIMS

m/z [TMS der + H]$^+$ 389.2494, calculated 389.2543 for $C_{19}H_{41}O_4Si_2$; EIMS m/z 181(6), 154(32), 142(18), 111(20), 97(39), 83(21), 69(47), 55(100); ^{1}H NMR δ ($CDCl_3$) 11.5 (2H, br, D_2O exchange), 2.7 (1H, dq, J=9.0, 7.1Hz), 2.5 (1H, ddd, J=9.0, 9.0, 4.7 Hz), 1.6 (2H, m), 1.2 (15 H, br s), 0.85 (3H, t, J=6.5 Hz); ^{13}C NMR δ $CDCl_3$ 182.3 (C), 182.1 (C), 47.8 (CH), 40.9 (CH), 31.8 (CH_2), 29.5 (CH_2), 29.3 (CH_2), 29.2 (CH_2), 29.1 (CH_2), 26.6 (CH_2), 22.6 (CH_2), 15.1 (CH_3), 14.1 (CH_3).

Physical/Chemical Data for Diol

Colorless oil; UV (MeOH) λ_{max} (ε) 210 (290); IR υ_{max} (cm^{-1}) (neat) 3328 br, 2922, 2854, 1715, 1456, 1378, 1035, 757, 721; HRCIMS m/z [M + H]$^+$ 217.2171 calculated 217.2168 for $C_{13}H_{29}O_2$; EIMS m/z 168(20), 154(02), 140(05), 125(08), 111(19), 97(37), 83(47), 69(88), 55(100); ^{1}H NMR δ ($CDCl_3$) 3.7 (2H, m), 3.5 (2H, m), 2.5 (2H, br, D_2O exchange), 1.7 (1H, m), 1.4 (1H, m), 1.2 (14H, br), 0.9 (3H, d, J=7.2 Hz), 0.85 (3H, t, J=6.6 Hz); ^{13}C NMR δ ($CDCl_3$) 65.2 (CH_2), 62.6 (CH_2), 44.1 (CH), 37.5 (CH), 32.3 (CH_2), 30.4 (CH_2), 30.0 (CH_2), 29.7 (CH_2), 29.5 (CH_2), 28.1 (CH_2), 23.1 (CH_2), 15.5 (CH_3), 14.5 (CH_3).

Physical/Chemical Data for Lactones

Light yellow oil; UV (MeOH) λ_{max} (ε) 212 (430); IR υ_{max} (cm^{-1}) (neat) 2923, 2854, 1777, 1456;HREIMS m/z **A**: M$^+$ 212.1775 calculated 212.1776 for $C_{13}H_{24}O_2$; **B**: M$^+$ 212.1770 calculated 212.1776 for $C_{13}H_{24}O_2$; EIMS m/z **A**: 212(02), 197(06), 113(53), 100(100), 85(82), 69(16), 55(33); **B**: 212(01),

181(01), 99(54), 83(32), 70(89), 55(100); ^{1}H NMR δ ($CDCl_3$, 500MHz) 4.4 (0.45H, dd, J=8.7, 7.7 Hz, **B**), 4.3 (0.55H, dd, J=8.5, 8.0 Hz, **A**), 3.8 (0.45H, dd, J=9.2, 8.7 Hz **B**), 3.7 (0.55H, dd, J=8.9, 8.5 Hz, **A**), 2.3 (0.55H, m, **A**), 2.2 (0.45H, m, **B**), 2.1 (1H, m), 1.7 (1H, m), 1.6 (2H, m), 1.5 (1H, m), 1.3 (10H, br), 1.2 (1.5H, d, J=6.5 Hz, **B**), 1.1 (1.5H, d, J=6.6 Hz, **A**), 0.9 (3H, t, J=6.3 Hz); ^{13}C NMR δ ($CDCl_3$,) 180.2 (C), 179.8 (C), 73.0 (CH_2), 72.1 (CH_2), 47.1 (CH), 44.2 (CH), 41.0 (CH), 36.5 (CH), 32.6 (CH_2), 32.2 (CH_2), 30.1 (CH_2), 30.0 (CH_2), 29.8 (CH_2), 29.6 (CH_2), 29.5 (CH_2), 29.4 (CH_2), 27.6 (CH_2), 27.2 (CH_2), 23.0 (CH_2), 17.3 (CH_3), 14.4 (CH_3).

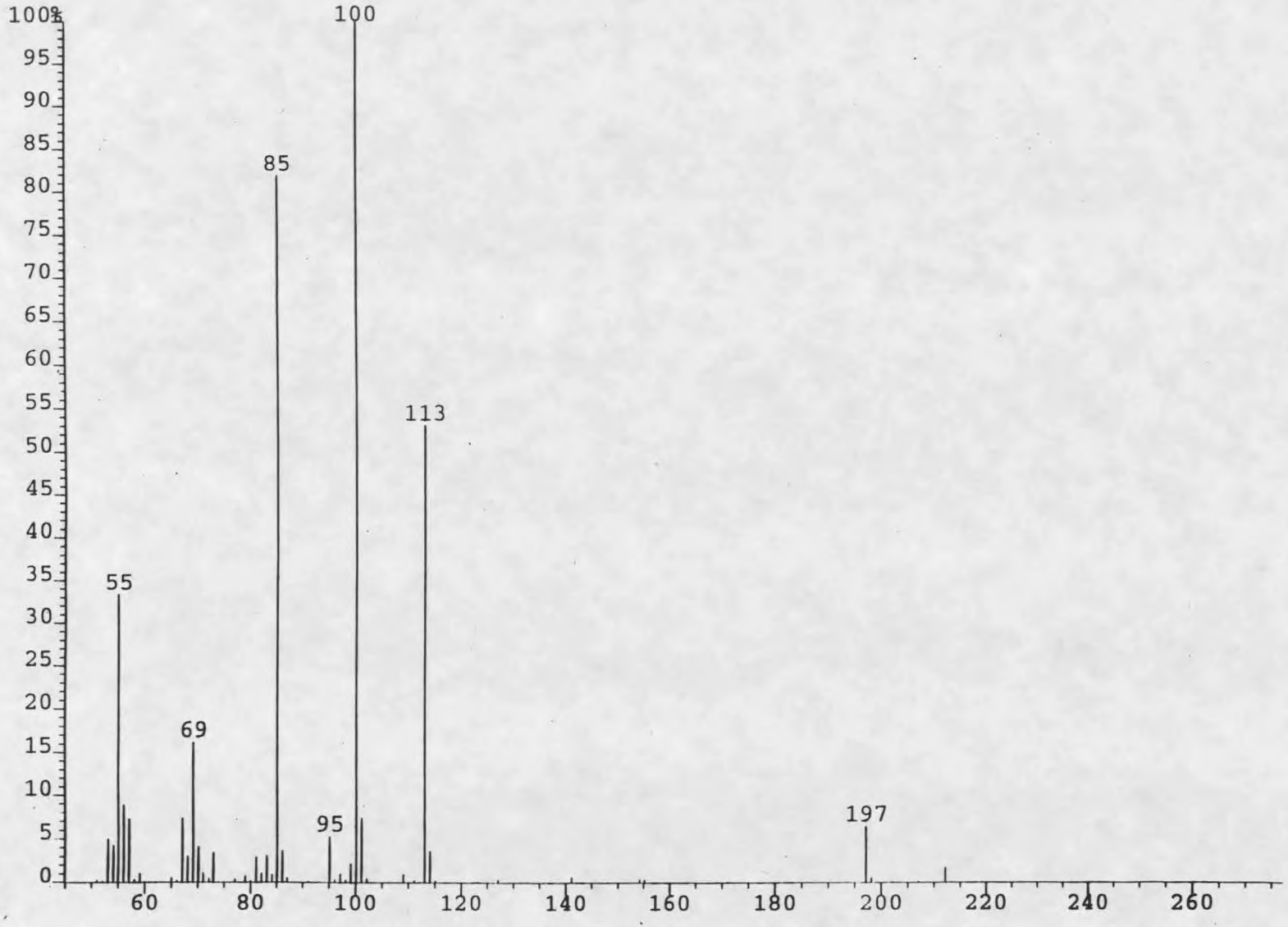

Figure 3.16 EIMS of lactone A

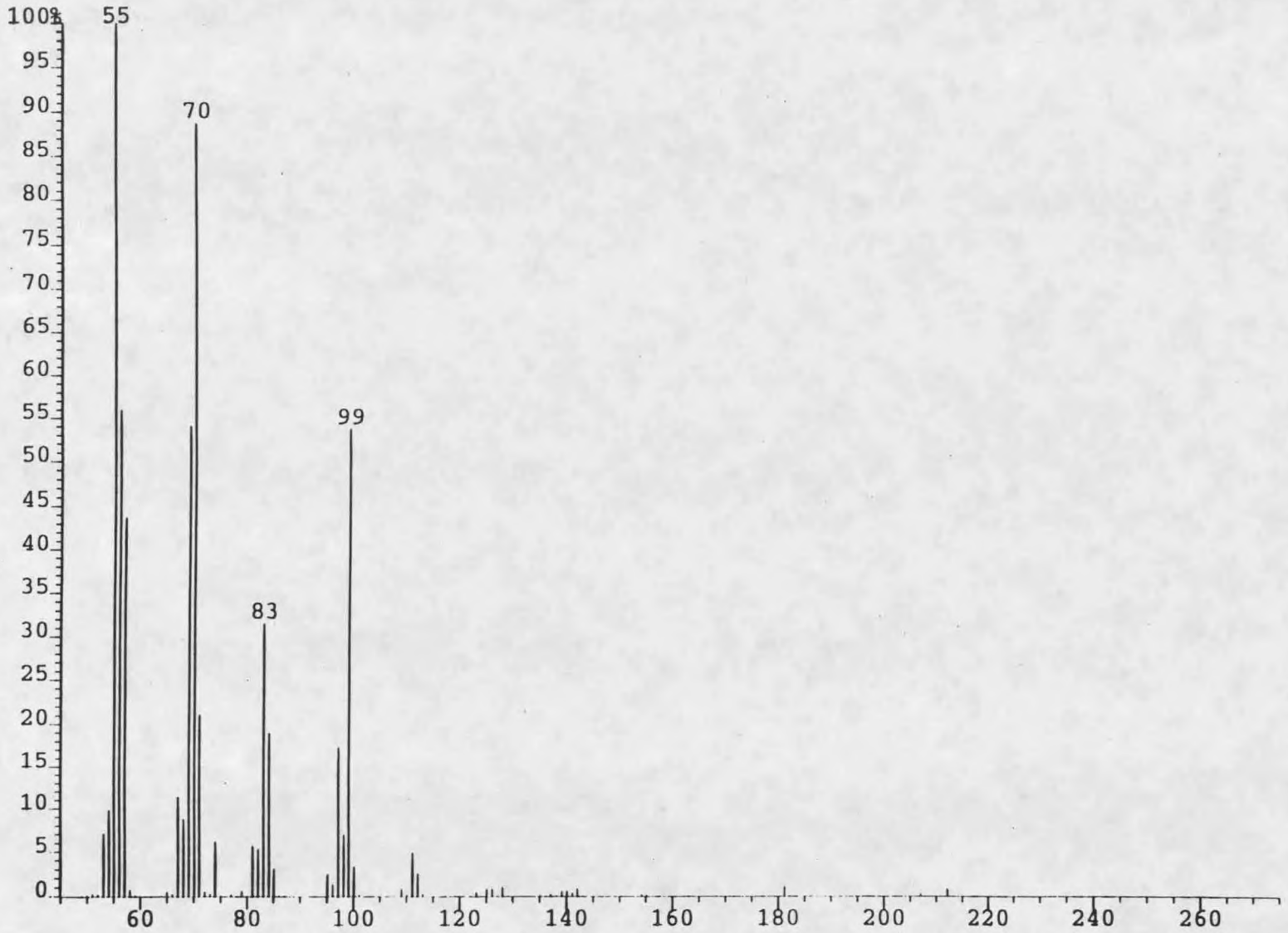

Figure 3.17 EIMS of lactone B

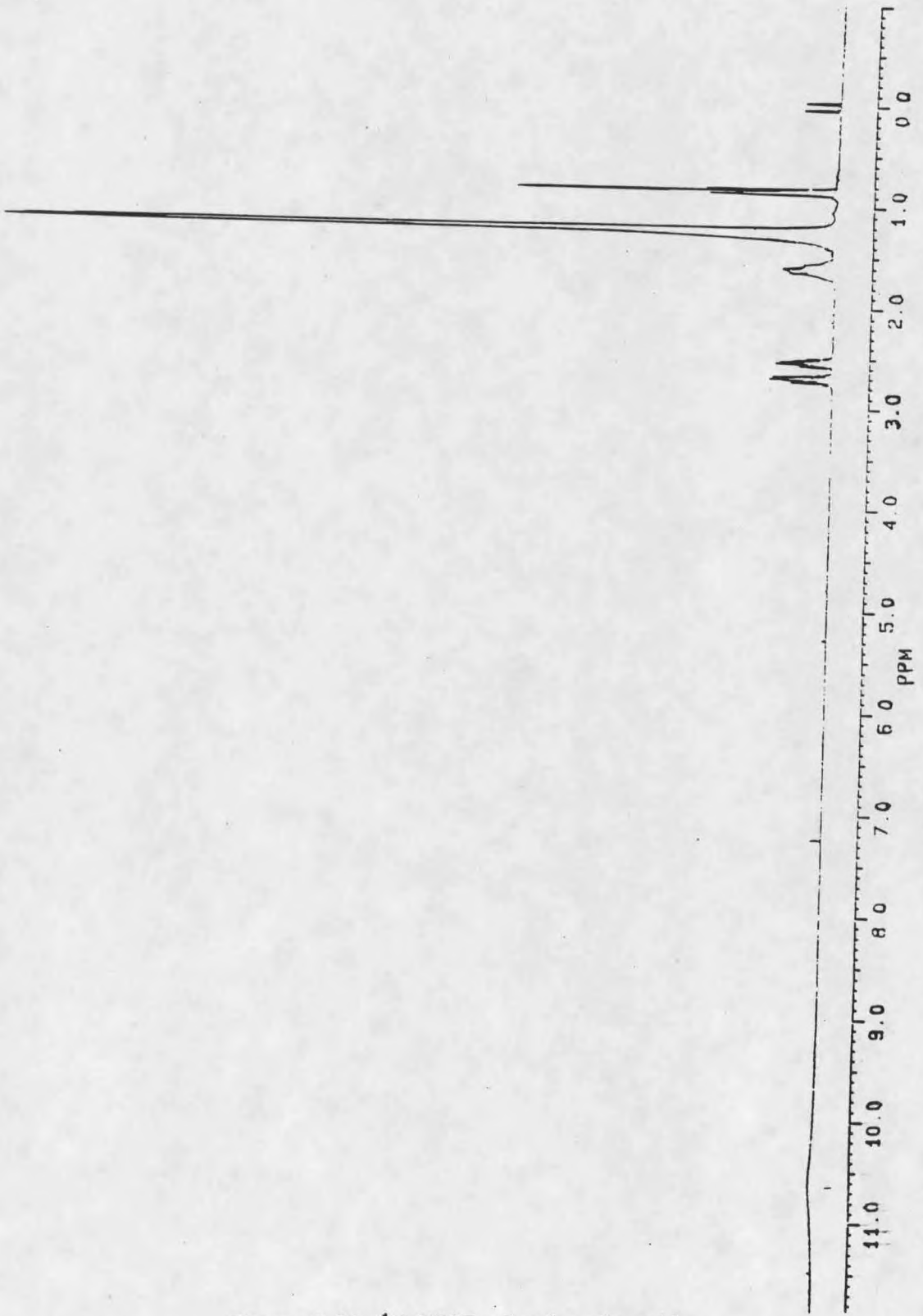

Figure 3.18 ^{1}H NMR of sphaeric acid

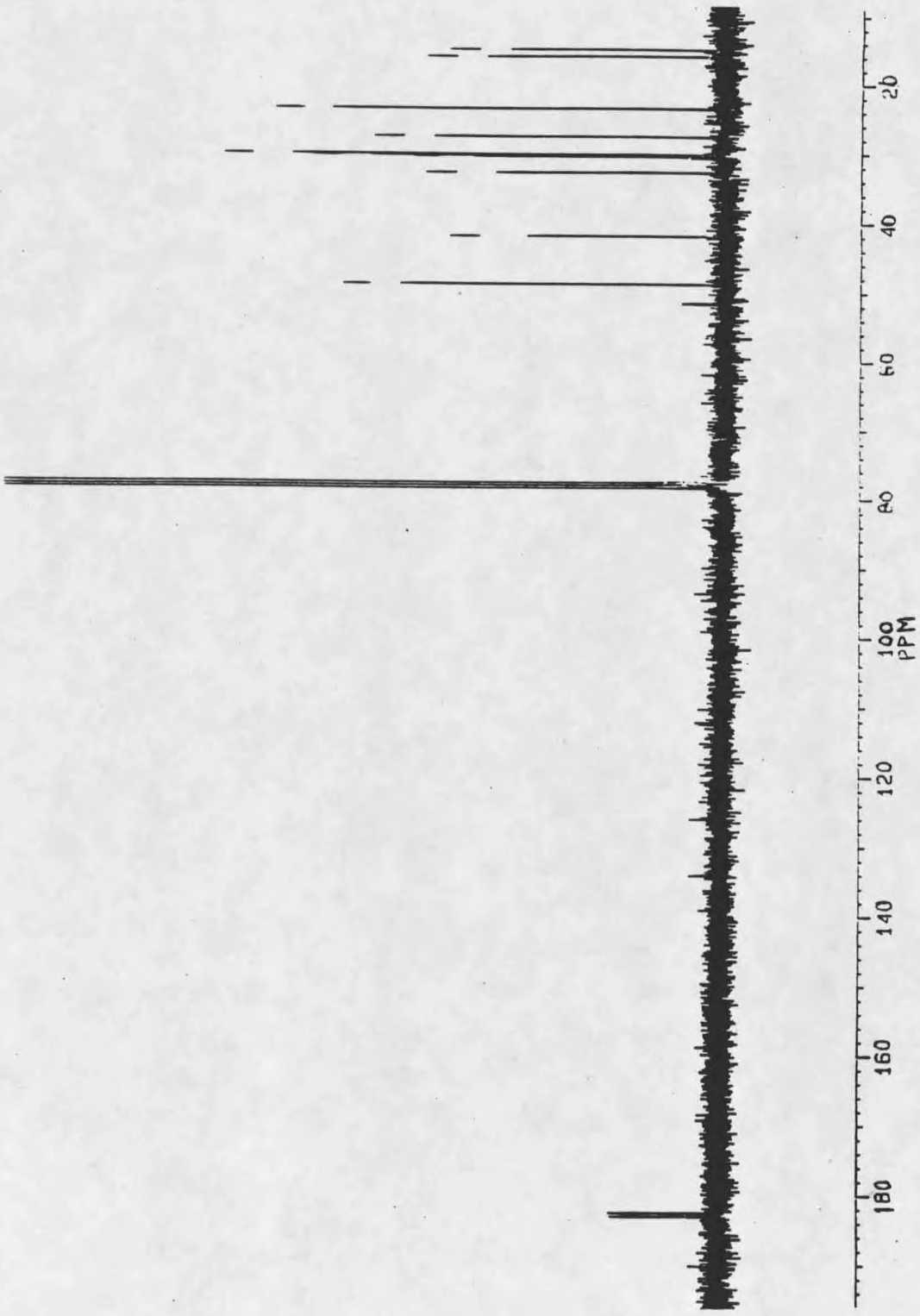

Figure 3.19 ^{13}C NMR of sphaeric acid

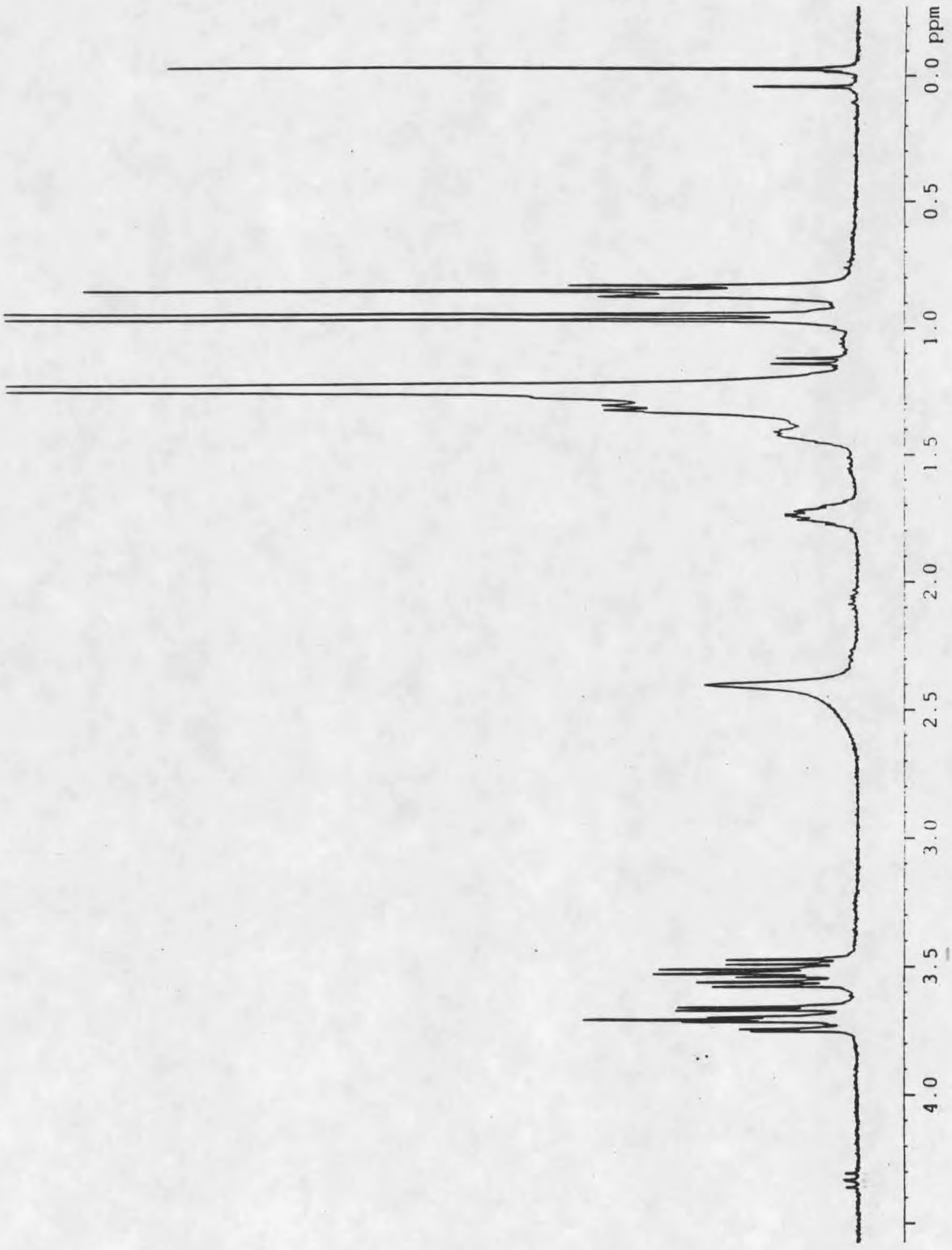

Figure 3.20 ^{1}H NMR of diol

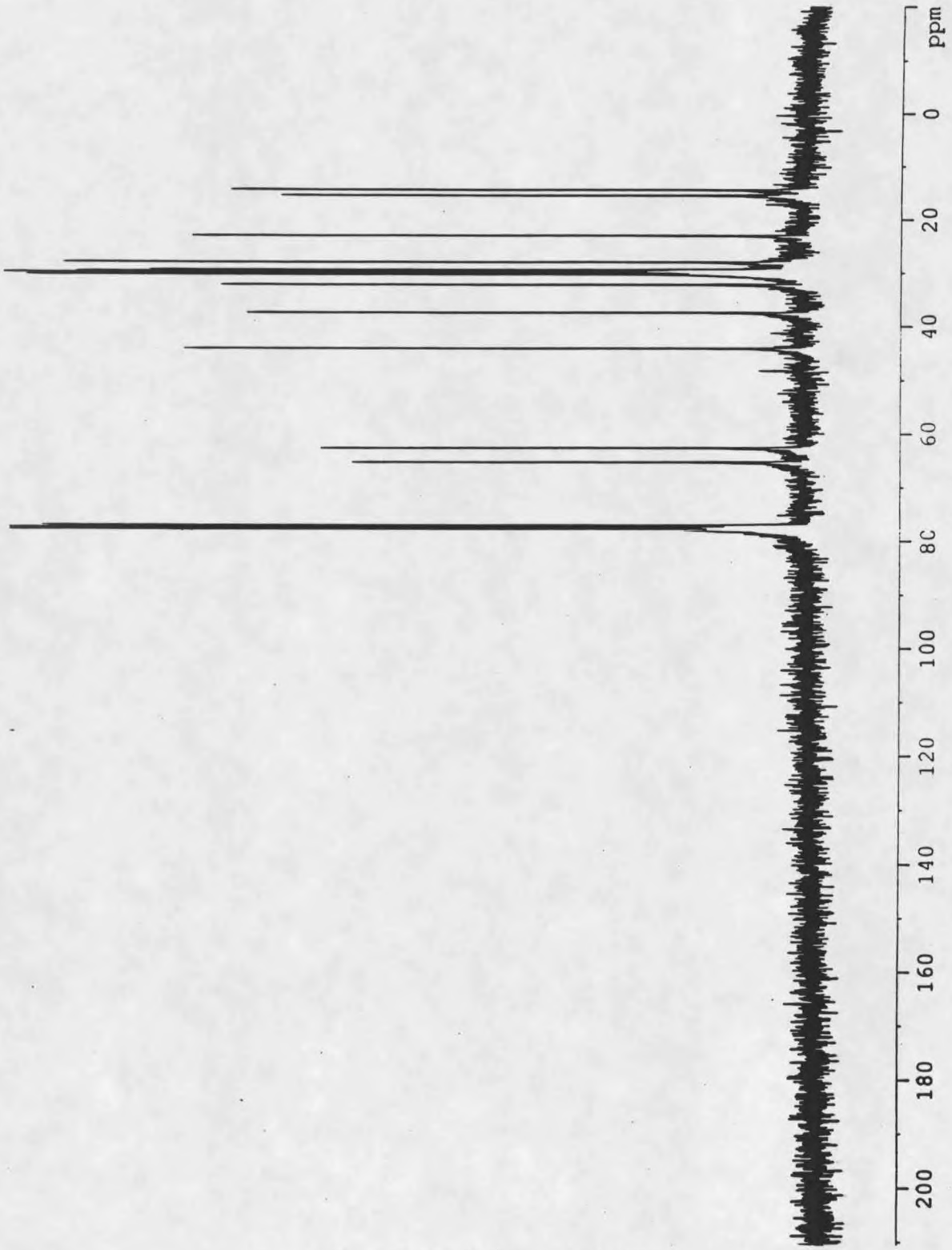

Figure 3.21 ^{13}C NMR of diol

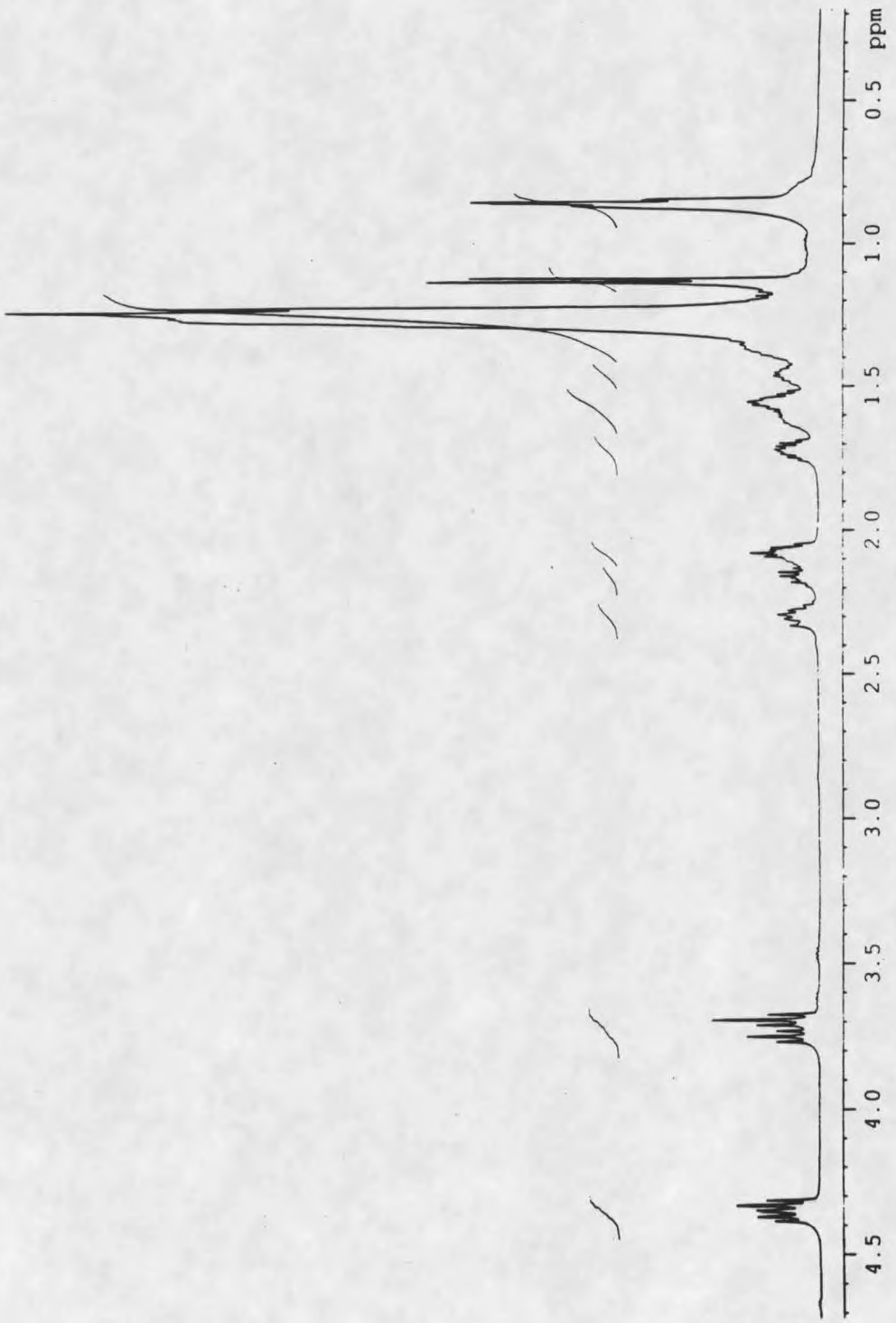

Figure 3.22 ^{1}H NMR of lactones

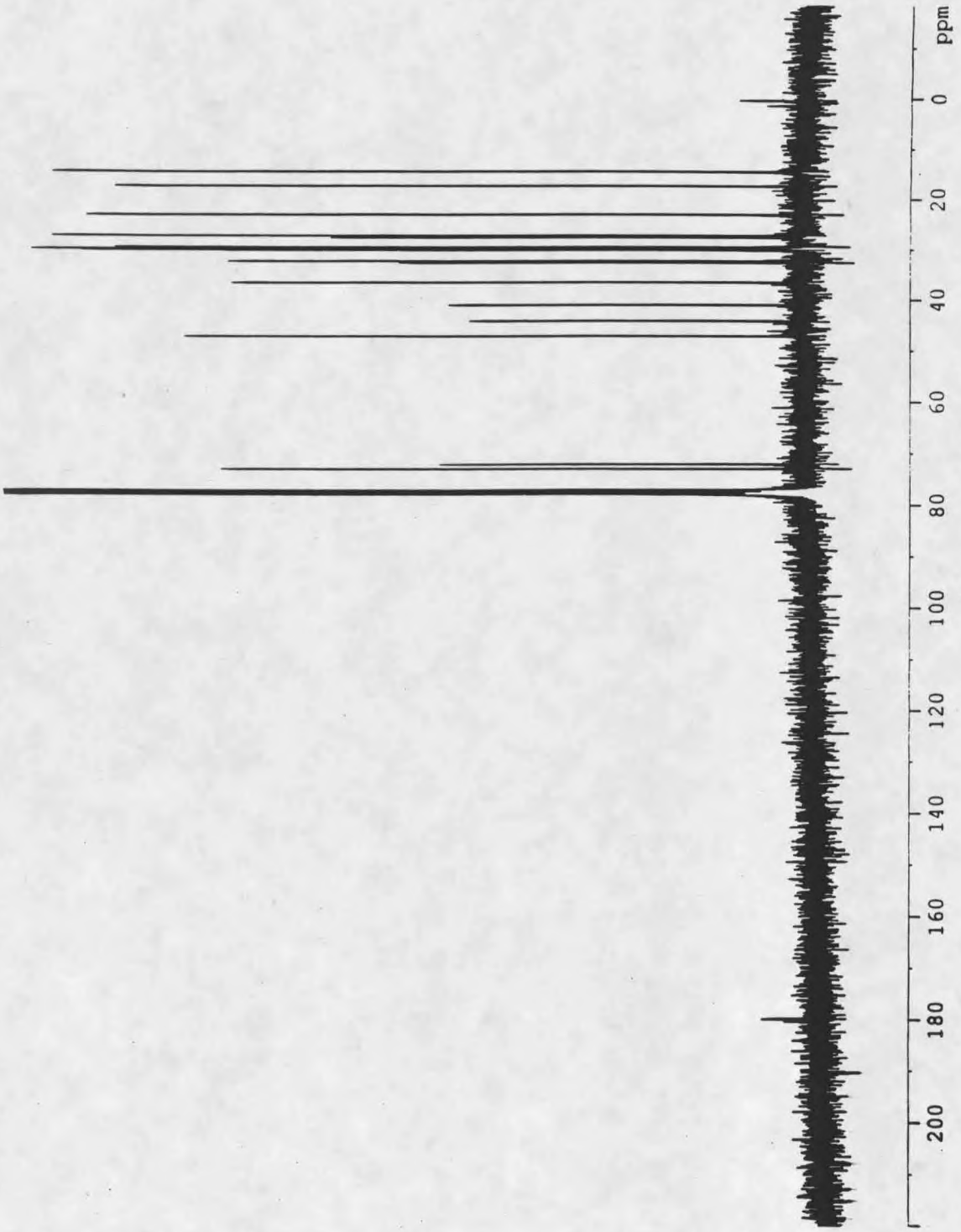

Figure 3.23 ^{13}C NMR of lactones

Chapter 4

DERIVATIVES OF SPHAERIC ACID

Many times a change in the structure of a molecule can have a great effect on its activity. This can be as subtle as a change in the configuration of a chiral center. For example, (R)-(-)-epinephrine is an active adrenal hormone, while (S)-(+)-epinephrine (Figure 4.1) does not correctly fit into the receptor enzyme's active site.[56] Other structural changes are also employed to effect the biological activity of compounds. For example, in studying the structure/activity relationship of 4-phenylethylaminoquinoline (Figure 4.2), Dreikorn et. al. synthesized analogues with structural modifications to study six areas:[57]

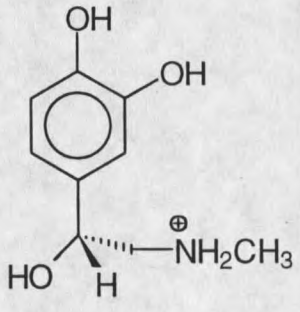

(R)-(-)-epinephrine

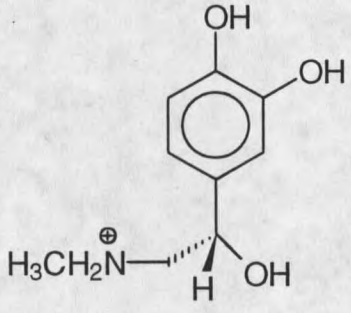

(S)-(+)-epinephrine

Figure 4.1 R and S Epinephrine

1) Positioning on the quinoline for the phenylethylamino group.
2) Varying the length of the alkyl (ethyl) chain.
3) Substitutions on the quinoline rings.
4) Substitutions on or replacement of the phenyl ring.
5) Substitution on the chain nitrogen or the alkyl chain.
6) Replacement of the chain nitrogen with other atoms.

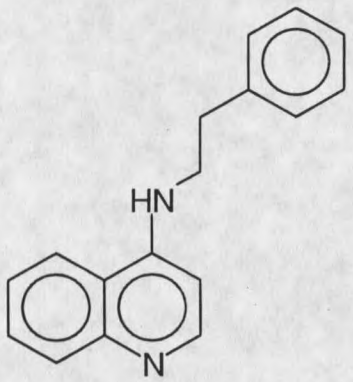

Figure 4.2 4-Phenylethylaminoquinoline

Included in the six categories of modifications were several general alterations. The electronic environment of the aromatic rings were altered by substitution with electron withdrawing groups (F, Cl, Br, I, CF_3) and electron donating groups (OH, OR, R). Steric factors were also considered in the substitutions of the phenyl ring by using increasingly bulky groups (H, Me, Et, i-Pr, t-Bu). The importance of the nitrogen in the alkyl chain was also investigated by replacing it with sulfur, sulfoxide, oxygen, and carbon. This can affect the electronic

environment of the quinoline ring, but could also indicate any hydrogen bonding requirements for activity.

In a similar manner, an investigation of the structure/activity relationship of sphaeric acid was conducted. In doing this, it was important to note its lipophilic properties. While its activity could be a result of interference in key metabolic pathways or enzyme inhibition, the most likely activity is an effect on cellular membranes. Lipid soluble antibiotics often effect the cellular membrane in one of three ways: those which appear to disorganize the membrane structure, those which inhibit a membrane bound protein, and those which change the permeability of the membrane to specific ions.[58]

In an attempt to study the structure/activity relationship of sphaeric acid, several derivatives were synthesized. An attempt was made to vary the polarity and charge of the polar end of sphaeric acid. This was accomplished by various methods including esterifications, amidifications, a reduction, and a subsequent oxidation. A series of bioassays were then conducted on sphaeric acid and the synthetic derivatives to test for any structure/function relationships.

The Derivatives

Methyl esters

The mono-methyl esters (Figure 4.3) were synthesized by two methods. Sphaeric acid was reacted with thionyl chloride in an attempt to make the diacid chloride. However, since the methyl ester singlets of the resulting products, at

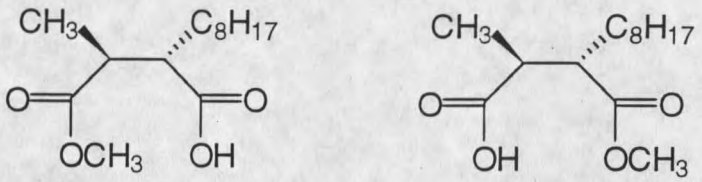

Figure 4.3 Mono-methyl esters of sphaeric acid
(Absolute stereochemistry unknown)

3.65 and 3.66 ppm, only integrated to three protons, it appeared that only the mono-methyl esters were formed. This can be explained by the formation of the five-membered anhydride ring upon reaction with the thionyl chloride instead of the diacid chloride (Figure 4.4). The mono-methyl ester was then formed by nucleophilic attack on one carbonyl by the methanol forming the ester which opened the ring giving the carboxylic acid. Sphaeric acid was also reacted with

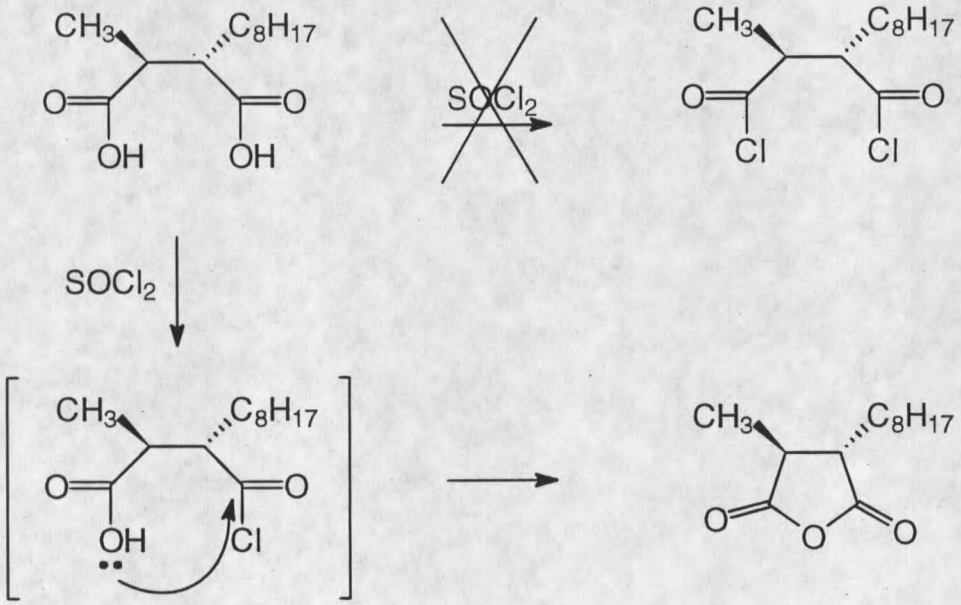

Figure 4.4 Formation of anhydride

diazomethane in an attempt to form the dimethyl ester, but again, the mono-methyl ester product was formed. It is possible, since the first step of the methylation involves the transfer of the proton from the carboxylic acid to the diazomethane[59], that the second proton was held too tightly between the two oxygens to transfer to the diazomethane (Figure 4.5). Another explanation could be that the acid was isolated as the mono-sodium salt, which would only react once to form the mono-ester mono-salt. However, the acid protons generally integrated to more than one proton (at least 1.5 protons) in the ^{1}H NMR, so it seems that at least some of the diester would be observed.

The other spectral data also supported the formation of the mono-methyl esters. The HREIMS analysis of the TMS (trimethylsilane) derivative gave a molecular formula of $C_{16}H_{31}O_4Si$, which corresponded to the TMS derivative of a mono-methyl ester of sphaeric acid with the loss of a methyl group. It is common in TMS derivatives for the molecular ion peak to be missing, but the M-15 peak from the cleavage of one of the silicon methyl bonds is often prominent.[60] The IR data included two carbonyl peaks at 1742 and 1704 cm^{-1}, corresponding to an ester and a carboxylic acid. The ^{13}C NMR data also supported the presence of two mono-methyl esters. There were two methyl signals at 52.2 and 52.0 ppm that correspond to carbons attached to oxygens. Additionally, there were four carbonyl signals at 176.3, 176.1, 175.9, and 175.7 ppm corresponding to the acid and ester carbons of each isomer. The

remaining proton and carbon signals corresponded very well to those of sphaeric acid.

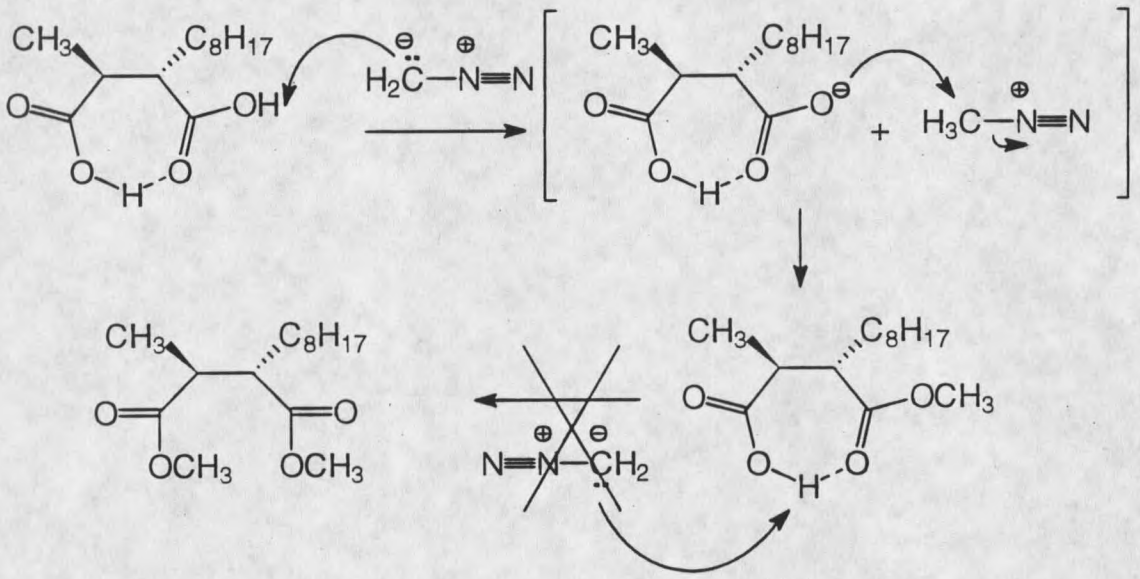

Figure 4.5 Diazomethane synthesis of mono-methyl ester

Ethyl esters

The two isomers of mono-ethyl esters of sphaeric acid (Figure 4.6) were formed in the same manner as the mono-methyl esters, using thionyl chloride to produce the cyclic anhydride. In this case, an attempt was made to try to produce the diacid chloride by using a ten-fold excess of thionyl chloride, but again, only the mono esters were recovered.

The HRCIMS gave a molecular formula of $C_{15}H_{32}NO_4$ which corresponded to the molecular ion plus NH_4 of a mono-ethyl ester of sphaeric acid. The IR data supported the mono-ester structure with two carbonyl signals at 1738 and 1704

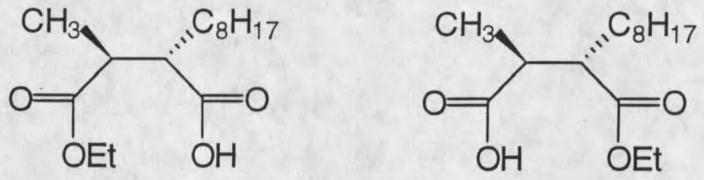

Figure 4.6 Mono-ethyl esters of sphaeric acid
(Absolute stereochemistry unknown)

cm^{-1} corresponding to an ester and a carboxylic acid. The proton NMR spectrum included two quartets at 4.13 and 4.14 ppm, corresponding to the methylenes on the oxygen of the ester and adjacent to a methyl group, which integrated to a total of two protons. The ^{13}C NMR also showed the methylene signals adjacent to an oxygen at 61.2 and 60.9 ppm and an the additional methyl signal at 14.7 ppm which was not present in sphaeric acid or the mono-methyl esters.

Isopropyl esters

The two isomers of mono-isopropyl esters of sphaeric acid (Figure 4.7) were formed in the same manner as the methyl and ethyl esters. The HRCIMS gave a molecular formula of $C_{16}H_{31}O_4$ which corresponds to the molecular ion plus a proton. The IR data supported the mono-ester structure with two carbonyl signals at 1732 and 1704 cm^{-1} corresponding to an ester and a carboxylic acid. The proton NMR spectrum included the septet at 5.0 ppm for the methine proton adjacent to the oxygen of the ester and two identical methyl groups. Additionally there was the doublet at 1.19 ppm of the methyl protons adjacent to

the above methine. The ^{13}C NMR showed the methine carbons adjacent to an oxygen at 68.6 and 68.4 ppm and the additional methyl signals at 22.1 and 22.0 ppm. There were also four carbonyl signals at 180.6, 179.7, 175.4, and 174.9 for the ester and carboxylic acid of each isomer.

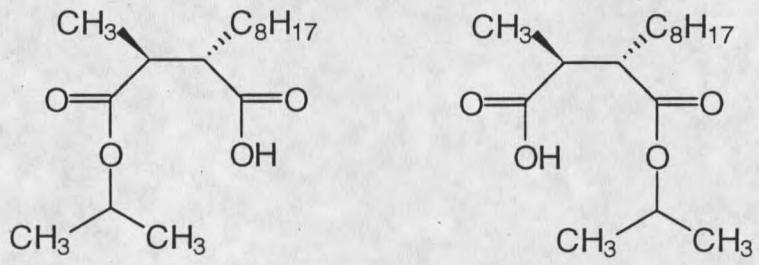

Figure 4.7 Mono-isopropyl esters of sphaeric acid
(Absolute stereochemistry unknown)

2-Chloroethyl esters

The two isomers of mono-2-chloroethyl esters of sphaeric acid (Figure 4.8) were formed in the same manner as the previous mono-esters. The HREIMS of the TMS derivative gave a molecular formula of $C_{17}H_{32}O_4SiCl$ which corresponded to the TMS derivative of a mono-2-chloroethyl ester of sphaeric acid minus a methyl group. The mono-chlorinated product was also supported by the presence of an M+2 peak of one third the intensity of the molecular ion peak. The IR data supported the mono-ester structure with two carbonyl signals at 1739 and 1707 cm^{-1} corresponding to an ester and a carboxylic acid. The proton NMR spectrum contained the two triplets, 4.3 and 3.6 ppm, of the 2-chloroethanol group, and the two methylene carbons are at 64.6 and 41.9 ppm.

in the ^{13}C NMR. The only evidence that both mono-esters were formed is the presence of three carbonyl signals at 180.1, 175.3, and 174.8 ppm instead of the two that would be present if only one isomer were formed.

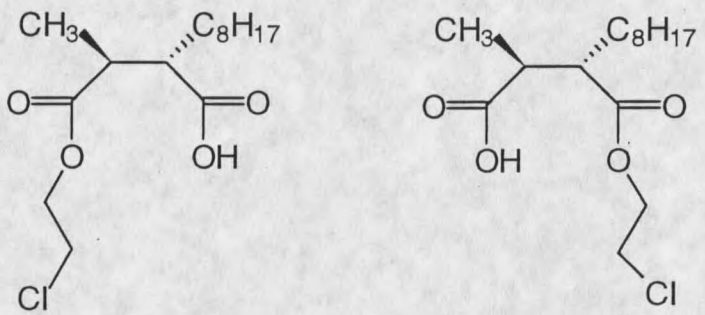

Figure 4.8 Mono-2-chloroethyl esters of sphaeric acid
(Absolute stereochemistry unknown)

2-Bromoethyl esters

The two isomers of mono-2-bromoethyl esters of sphaeric acid (Figure 4.9) were formed in the same manner as the previous esters. The HREIMS of the TMS derivative gave a molecular formula of $C_{17}H_{32}O_4SiBr$ which corresponded to the TMS derivative of a mono-2-bromoethyl ester of sphaeric acid minus a methyl group. The mono-brominated product was also supported by the presence of an M+2 peak of intensity equal to the molecular ion peak. The IR data supported the mono-ester structure with two carbonyl signals at 1738 and 1708 cm^{-1} corresponding to an ester and a carboxylic acid. The proton NMR spectrum contained the two triplets, 4.4 and 3.5 ppm, of the 2-bromoethanol group, and the two methylene carbons are at 64.5 and 64.3 ppm in the ^{13}C

NMR. The ^{13}C NMR data supported the presence of the two isomers with the four carbonyl signals at 180.4, 179.6, 175.2, and 174.6 ppm for the ester and acid of each isomer. Additionally, there were two signals for each of the methines (47.5/47.7 ppm and 40.9/41.0 ppm) and two signals for the methyl group (14.7/14.8 ppm) adjacent to one of the methines.

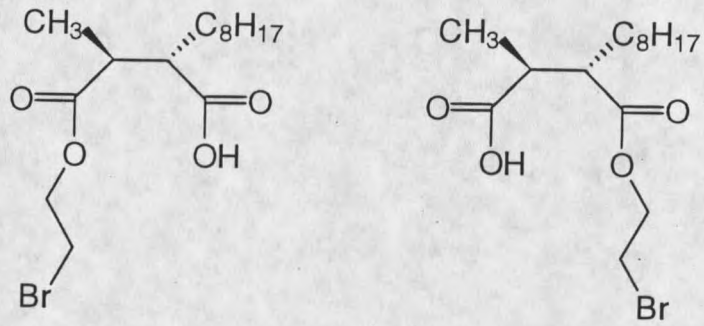

Figure 4.9 Mono-2-bromoethyl esters of sphaeric acid
(Absolute stereochemistry unknown)

Mono-amide

The two isomers of the mono-amide derivative of sphaeric acid (Figure 4.10) were made in a similar method to the mono-esters. The cyclic anhydride was produced by reaction of the diacid with thionyl chloride, and then allowed to react with the ammonia in solution.

The mass spectral data was unavailable for these compounds. The IR data supported the mono-amide structure by showing two carbonyl peaks at 1714 cm^{-1} and a shoulder at 1650 cm^{-1} corresponding to an acid and an amide. The proton NMR, as expected, was very similar to that of sphaeric acid, with no additional peaks. The ^{13}C NMR was also very similar to that of sphaeric acid,

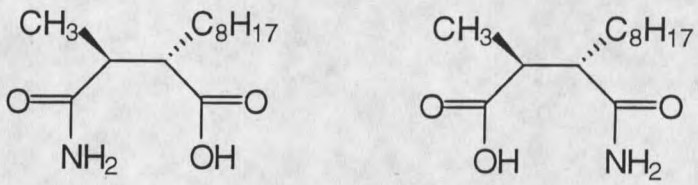

Figure 4.10 Mono-amides of sphaeric acid
(Absolute stereochemistry unknown)

but the presence of the two isomers was suggested by the pairs of signals for the methines at 48.7/49.0 ppm and 42.1/42.4 ppm.

Mono-methyl amide

The two isomers of the mono-methyl amide of sphaeric acid (Figure 4.11) were made in a manner similar to the mono-amide derivatives. The CIMS contained an M+1 peak at 258, and a base peak at 257 which results from the loss of a hydrogen atom α to the nitrogen of the amide (i.e. from the N-methyl). The IR data supported the mono-amide structures with two carbonyl signals at 1650 and 1574 cm^{-1} corresponding to an amide and a carboxylate anion. The proton NMR showed the presence of the two N-methyl signals of the amides at 2.71 and 2.70 ppm. These combined to an integration of only three protons since only the mono-amide was being formed. The ^{13}C NMR also supported the formation of the mono-methyl amides. The two methyls attached to the amide nitrogens appeared at 25.7 and 25.8 ppm. The four carbonyl signals, 183.6, 182.6, 178.8, and 178.1 ppm, corresponded to the acid and amide of each isomer. Additionally, there were pairs of signals for each of the methines

(52.8/51.2 ppm and 45.8/44.1 ppm) as well as for several of the other carbon signals.

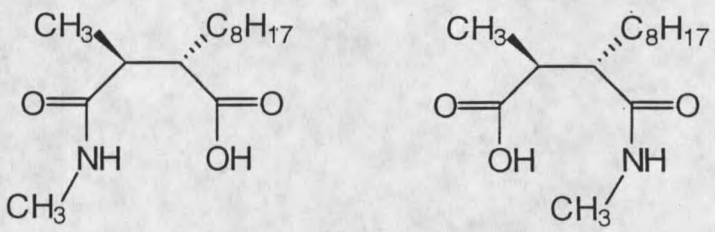

Figure 4.11 Mono-methyl amides of sphaeric acid
(Absolute stereochemistry unknown)

Phenyl imide

The phenyl imide of sphaeric acid (Figure 4.12) was made in the same manner as the other mono-amides. The HRCIMS gave a molecular formula of $C_{19}H_{28}NO_2$ corresponding to the molecular ion plus a proton. The HREIMS gave a molecular formula of $C_{19}H_{27}NO_2$ corresponding to the molecular ion. The broad, strong peak at 3380 cm^{-1} in the IR was believed to come from the O-H stretch of the water molecule produced in the dehydration of the mono-amides (Figure 4.13)

The IR showed only a single carbonyl peak at 1701 cm^{-1}. The proton NMR showed the aromatic protons of the phenyl ring at 7.3-7.5 ppm with the appropriate splitting for a mono-substituted benzene. The ^{13}C NMR was very clean without any of the multiple signals observed in the other derivatives. There were only two carbonyl signals (179.3 and 178.6 ppm) and two signals

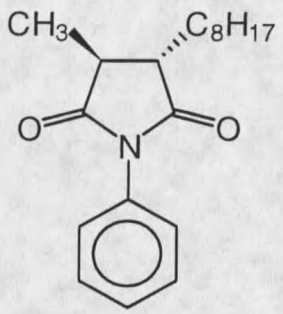

Figure 4.12 Phenyl imide of sphaeric acid

for the methines (48.5 and 41.5 ppm). This suggested that only one isomer, the phenyl imide, was being formed instead of the multiple isomers of the mono-amides observed in the other derivatives.

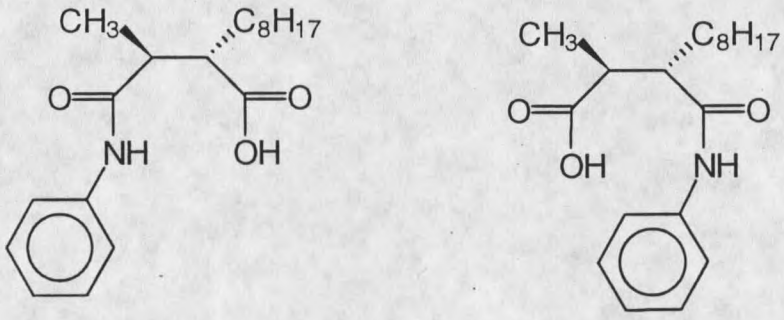

Figure 4.13 Mono-phenyl amides of sphaeric acid

Mono-glucosamides

The two isomers of the mono-glucosamide derivatives of sphaeric acid (Figure 4.14) were made in a manner similar to the other mono-amides. There was also some evidence that a small amount of mono-glucosamine esters were